1957-05

Fuel vaporization in the pre-ignition zone of a gas turbine combustion chamber.

Hess, John A.

University of Minnesota, 1957.

FUEL VAPORIZATION IN THE PRE-IGNITION ZONE OF A GAS TURBINE COMBUSTION CHAMBER

A Thesis Submitted to the
Faculty of the Graduate School of the
University of Minnesota

By

John A. Hess
Lt. U. S. Navy

In Partial Fulfillment of the Requirements
for the Degree of
Master of Science in Aeronautical Engineering

May 1957

ACKNOWLEDGEMENTS

I wish to express my appreciation to all the people who influenced this thesis. My sincere thanks to my adviser, Professor Thomas E. Murphy, for his advice and guidance throughout this work; to Lt. J. R. Hawvermale U.S.N. for his ready ear and willing hand; to Mr. W. J. Alden for his machine shop experience and advice; and to the professors of the University of Minnesota for their deep interest in the problems of the student.

Last but not least, I express my appreciation to my family for their patience and understanding throughout the past three years of advanced academic study.

This project was sponsored by the U. S. Navy under the supervision of the U. S. Naval Postgraduate School, Monterey, California.

John A. Hess
May, 1957

FUEL VAPORIZATION IN THE PRE-IGNITION ZONE
OF A GAS TURBINE COMBUSTION CHAMBER

SUMMARY

An investigation of the effect of the variables, inlet air temperature, air pressure, air velocity, fuel-air ratio and axial distance from the injector on benzene fuel vaporization was conducted under conditions simulating those of a gas turbine combustion chamber in the pre-ignition zone.

Determination of the percentage of fuel mass vaporized was achieved by solving the heat balance equation for the vaporization process using temperature measurements obtained from two shielded thermocouples in the benzene spray.

For injection parallel to the air flow and downstream, it was found that fuel vaporization is increased with increasing temperature and axial distance from the injector. Fuel vaporization decreases with increasing inlet air pressure, inlet air velocity and fuel-air ratio. An empirical formula to show the relative effects of each parameter was found to be

$$\frac{N}{100 - N} = K(T_a)^{4.00}(P_a)^{-0.84}(V_a)^{-1.43}(F/A)^{-0.27}(L)^{1.23}$$

degrees Rankine, inches Hg. absolute, feet per second,

inches. The expression for the axial distance effect is a maximum value, being an approximation instead of an exact result.

This investigation was done by Lt. John A. Hess, USN at the University of Minnesota, Minneapolis, Minnesota, as partial fulfillment of the requirements for the degree of Master of Science in Aeronautical Engineering.

FUEL VAPORIZATION IN THE PRE-IGNITION ZONE OF A GAS TURBINE COMBUSTION CHAMBER

INTRODUCTION

The chemical and mechanical processes of fuel vaporization in a gas turbine combustion chamber hold many complex secrets, yet to be revealed to engineers. A thorough understanding of how to achieve maximum vaporization of an injected fuel in a minimum of combustion chamber length, and the parameters affecting vaporization would permit the engineer to design the most efficient combustion chamber for all flight conditions.

In a gas turbine, the fuel is injected under pressure through an atomizing nozzle. It enters the combustion chamber or flame tube as a ligament or sheet. This sheet is broken up by the air stream into droplets of varying size, which absorb heat from the air stream, and radient energy from the flame body. The equilibrium temperature to which the droplets heat is the wet bulb temperature of the fuel under the ambient air pressure and temperature conditions. The larger droplets heat up more slowly than the smaller ones and also slow down less rapidly in the air stream.

The smaller droplets vaporize quickly and form a cloud of fuel vapor which moves downstream in the air flow. The mass of vapor given away by the larger droplets adds to this vapor cloud. Somewhere in the chamber a combustible mixture is formed. If this mixture is not then ignited by some outside source, it continues to be heated to its self-ignition temperature.

By definition, the physical portion of ignition delay extends from the time of injection to the time when the combustible mixture of fuel and air is heated to its self-ignition temperature. The fuel droplets reach their wet bulb temperature asymtotically with time. When the wet bulb temperature is attained, the process is assumed to enter a steady state. All events prior to this time are in the unsteady state.

To simplify the problem of analyzing the events in vaporization, some experiments have been conducted using a single fuel droplet in an air stream. El Wakil, Ref. 1, worked with a single droplet analysis to determine the importance of the unsteady state and the time of heating or cooling of fuel droplets to the wet bulb temperature. He found that after the droplets reached equilibrium temperature, the heat and mass transferred to and away from the droplets are functions only of the radius and velocity of the droplet. El Wakil also found that highly volatile fuel droplets of given size require less time to reach equilibrium for the same initial conditions than low volatility

droplets.

Two general methods of analytical calculation of vaporization rates of pure droplets may be used. Mass transfer equations employ the difference between the partial pressure of the vapor at the droplet surface and the ambient air. The other method is based on heat transfer equations. The driving potential is the difference between the air temperature and the surface temperature of the liquid.

Ingebo, Ref. 2, in his investigation of vaporization rates of pure liquid droplets used the heat transfer equations. This again was an investigation using only a single droplet in an airstream.

Bahr, Ref. 3, and Foster and Ingebo, Ref. 4, in their work simulated a ramjet combustor into which iso-octane in Bahr's case and JP-5 for Foster and Ingebo was injected contrastream. An NACA mixture analyzer was used to analyze probed samples of the fuel-air mixture.

Foster and Ingebo, Ref. 4, used the same equipment as Bahr, Ref. 3, and found that the percent evaporated of both iso-octane and JP-5 could be approximated by an empirical formula for the range investigated by

$$N = K\Delta T^{0.28} L^{0.33} \left(\frac{U_a + U_f}{100 + U_a} \right)^2 \qquad (1)$$

where N is the percent evaporated, K is a constant depending on the fuel used, ΔT is the difference between the air temperature and the wet bulb temperature of the fuel, L is

the distance downstream from the injector, and U_a and U_f are the air and fuel velocities respectively.

Bahr presented his results in the following manner:

$$\frac{N}{100 - N} = 9.35 \left(\frac{T_a}{1000}\right)^{4.4} \left(\frac{V_a}{100}\right)^{0.80} P_a^{-1.2} P_f^{0.42} L^{0.84} \quad (2)$$

where N is again the percent evaporated, T_a is the airstream temperature, V_a is the airstream velocity, P_a is the static air pressure, P_f is the fuel injection pressure and L the axial length downstream from the injector.

Apparently then the percent of a given fuel evaporated can be represented by an empirical equation with the parametric exponents being constant and the constant K in the equation being a function of the fuel.

This investigation concerns itself with determining an empirical relationship for the percent of benzene fuel evaporated with the parameters investigated being, airstream temperature, stream pressure, stream velocity, fuel-air ratio and axial length from the injector.

$$N = f(T_a, P_a, V_a, F/A, L) \quad (3)$$

SYMBOLS

A	Area, ft^2
c_p	Specific heat at constant pressure, BTU/lb-^oF
D	Diameter, ft.
e	Emissivity
F	Farenheit
F/A	Fuel-air ratio, dimensionless
G	Weight velocity, lb/hr-ft^2
H_v	Latent heat of vaporization, BTU/lb
h	Heat transfer coefficient, BTU/hr-ft^2-^oF
K	Arbitrary constant to fit equation to which applied
k	Thermal conductivity, BTU-ft/hr-ft^2-^oF
L	Length, inches
$\dot{m}$	Mass flow, lbs/sec
P	Pressure, inches of mercury absolute
q	Rate of heat flow, BTU/hr
T	Temperature, ^{o}Rankine
t	Temperature, ^oF
V	Velocity, ft/sec
X	Percent of fuel mass vaporized
μ	Absolute viscosity, lb/hr-ft
ρ	Density, lb/ft^3

Subscripts

1	Initial condition
2	Final condition

Subscripts continued

a	Air
c	Convection
f	Fuel
gr	Gas radiation
k	Conduction
p	Pyrometer
r	Radiation
s	Shield

EQUIPMENT

General: The equipment consisted of an insulated heated wind tunnel powered by a Lycoming air cooled tank engine driving an aircraft type centrifugal supercharger which pulled the air through the test section. The tunnel was mounted vertically, being hung from the overhead of the test cell on four half inch steel bolts. Fuel was injected into the test section by an atomizing nozzle and temperatures in the spray were measured with two shielded thermocouples, one located at about the half way point along the test section and the other at the exit.

Test Section: The test section was four by four inches square and twenty inches long. Two sides were made of one-half inch pyrex glass for visual observation of the fuel spray, the other two sides were of one-quarter inch cold rolled carbon steel. Holes were drilled at intervals along the steel plates as shown in Fig. 1 to permit measurement of the static pressure along the test section and insertion of thermocouples and total pressure probes through threaded stuffing boxes.

Fuel System: Technical Benzol fuel was stored in a five gallon tank pressurized with carbon dioxide gas. This tank

was immersed in a larger tank containing water to keep the fuel temperature as constant as possible. Fig. 2 shows the arrangement. From the tank, the benzol fuel passed through two filters, one-quarter inch copper tubing, a calibrated flow meter, various valves and was introduced into the test section through a Hago atomizing nozzle, located at the inlet to the test section and spraying downstream along the longitudinal axis of the test section. The nozzle was rated at nine gallons per hour with a thirty degree cone angle at 100 pounds per square inch differential pressure for fuel having a viscosity of 35 seconds Saybolt. The nozzle distributed the atomized fuel particles uniformly throughout the entire spray. Fig. 3 shows this distribution.

The one-quarter inch copper tube fuel line was led through a one-half inch pipe in the tunnel settling chamber with cooling water flowing around the fuel line inside the tunnel. This kept the benzene fuel at a low temperature for injection.

Tunnel: The tunnel layout is as shown in Figs. 4, 5 and 6 with Figs. 7, 8, 9 and 10 showing detailed views. Air flow was through the inlet valve at the top, through twelve chromolox 230 volt, 2450 watt finstrip electric heaters, the settling chamber, contraction nozzle, test section and thence to the compressor and exhausted to the atmosphere.

The electric heaters were wired in parallel across 230 volt bus lines and were individually fused and switched.

The heaters were mounted normal to the air flow in four rows of three each in the tunnel. The three heaters in the top row were series wired to rheostats to permit fine temperature control of the inlet air.

Two 50 mesh screens were installed in the settling chamber to damp out turbulence in the moving air before it reached the test section.

Downstream of the test section an air bleed valve was installed to control the static pressure in the test section. Closing this valve increased vacuum in the test section.

Instrumentation: Temperatures of the air and spray mixture flowing through the test section were read by shielded thermocouples as shown in Figs. 11 and 12, one located at station 10, 8.55 inches from the nozzle, and another at station 18, 16.4 inches from the nozzle. These thermocouples were connected to a direct reading potentiometer through a multiple switch panel. The potentiometer could be read to an accuracy of one degree Farenheit.

Pressures were read on a manometer board using a 30 degree inclined tube manometer containing alcohol for dynamic pressure and an adjustable scale mercury manometer for static pressure. The barometric pressure could be set on the static pressure manometer so it read absolute pressure. Dynamic pressure was read at the test section entrance. Static pressure was read at the half way point, station 10, in the test section. The dynamic pressure scale was graduated in .05 inch increments. The static

pressure scale was graduated in tenths of inches.

Fuel pressure was read from a gage located just before fuel was piped into the tunnel. Fuel flow rate was read from a calibrated flow meter capable of being read to an accuracy of one-tenth of a gallon per hour.

A thermocouple sensing element was located at the fuel probe cooling water exit to read water exit temperature to be used in determining the fuel temperature at injection.

Thermocouples: The thermocouples used to measure the temperatures in the test section are shown in Figs. 11 and 12. All were made of 0.010 inch iron-constantan wire, mercury arc-welded at the temperature sensing junction. The wire was inserted through a hypodermic needle tubing having an outside diameter of .082 inches. The tubing was fitted to a stuffing box for screwing into the test section.

Two thermocouples shown at the left of Fig. 11, were used throughout the testing because they provided the most protection from wetting by the liquid fuel. These thermocouples were constructed of two concentric cylinders with a cap about one-eighth inch ahead of the cylinders. The whole arrangement was held together by piano wire, silver soldered to the hypodermic needle tubing. The thermocouple sensing junction was located inside the second cylinder. The concentric cylinder arrangement was used to reduce radiation of the temperature sensing element to the cool walls of the outer shield. Fig. 12 shows the detailed thermocouple con-

struction.

The configuration on the right in Fig. 11 was used to measure shield temperature in the spray to attempt to determine the thermocouple error. Two thermocouples were located on this instrument, one attached to the shield to measure its temperature and one behind the shield to measure air temperature in the spray.

More will be said about thermocouple construction and their errors later on.

Equipment Calibration: Figs. 13 and 14 show nomographs constructed to determine tunnel velocity and air mass flow rate.

Fig. 15 shows the calibration of the Hago fuel nozzle. Fig. 16 gives the benzene flow rates for the flow meter graduated scale readings. The flow meter was designed for gasoline so had to be calibrated for benzene.

Fig. 17 shows the velocity profiles obtained in the test section.

Fig. 18 shows the temperature profiles obtained in the test section using various heater combinations.

The range of the variables temperature, pressure, velocity and fuel pressure were:

Air Temperature	85 to 400 degrees F.
Air Pressure	atmospheric to 8 inches vacuum
Air Velocity	50 to 250 feet per second
Fuel Pressure	0 to 150 pounds per sq. in. gage

PROCEDURE

The variables chosen for investigation were inlet air temperature, static air pressure, inlet air velocity, fuel-air ratio and axial distance from the injector. To determine the effects of one variable on fuel vaporization, all were held constant except the variable being investigated during any one run.

From the temperature profiles made in the calibration of the tunnel, it was found that a point 1.45 inches from the left wall of the tunnel test section could be taken as the average temperature in the test section at stations 10 and 18. This permitted measuring the temperature in the spray at only one point at stations 10 and 18 since the spray nozzle gave a uniform distribution. This single point then was representative of the average conditions in the tunnel at that axial station.

Fuel-air ratio was chosen as approximately stoichiometric, .075, and delivery rate at 1.15 pounds per minute with air mass flow adjusted to make the ratio .075. Static pressure when constant was held at 27 inches of mercury absolute. When temperature was held constant, it was held as close to the neighborhood of 300 degrees Farenheit as

possible. The heaters were always used in groups of three, since this comprised a complete row, giving uniform heating of the air.

Before each run, the inclined tube manometer used to measure dynamic pressure was zeroed and the mercury static pressure manometer set to barometric pressure. The potentiometer was zeroed and all thermocouple temperatures checked to see that the thermocouples were operating before starting the tunnel. The benzene fuel tank was refilled at the end of the previous run and allowed to sit in its water bath so the fuel temperature was stabilized.

When all preparations had been completed, the tunnel was started and the desired heaters switched on. When any heat was on in the tunnel, the cooling water was always circulated around the fuel pipe in the tunnel. Air temperature, pressure and velocity were then adjusted to the desired values. About thirty minutes had to be allowed for the tunnel to heat to a high temperature and stabilize. Less time was needed of course for lower temperatures.

All air temperatures before and during injection of fuel were read by the shielded thermocouples placed 1.45 inches from the left wall at stations 10 and 18. Static pressure was read at station 10. Dynamic pressure was read at the entrance to the test section.

When all appeared to be ready for a data reading, the fuel valve was opened and fuel injected. With the valve open, the fuel flow rate was adjusted to give the proper

reading on the fuel flow meter. The fuel valve was then closed and the temperature allowed to stabilize again, no data being taken as yet.

When the temperature had been constant for several minutes, all was then ready for a data reading. The air temperatures at stations 10 and 18, dynamic pressure at the inlet and static pressure at station 10 were read and recorded. The fuel valve was then opened injecting benzene fuel into the test section and the fuel flow meter reading noted to see that it was proper. After about thirty seconds, the thermocouple temperatures remained steady, having dropped to a lower value during injection, and temperature readings were taken at stations 10 and 18 in the spray. The fuel inlet valve was then closed. This procedure was repeated again for the next desired data point.

During all the runs for varying air temperature, data was first recorded at the low temperature with the temperature being increased thereafter. Pressure runs were made with both increasing and decreasing series runs. One way was as easy as the other. All fuel-air ratio runs were made starting with a low fuel-air ratio and increasing. This again was for convenience because the fuel flow was increased by increasing the carbon dioxide pressure on the fuel tank. The velocity runs were made starting with a low velocity and increasing. This was because velocity was increased by increasing the compressor rotation rate and with increasing velocity, more heat had to be applied to

keep the temperature constant. Also, fuel injection pressure was increased with increasing air velocity to maintain constant fuel-air ratio.

Fine temperature control was achieved by varying the resistance in the heater circuit containing heaters one through three. These heaters were always in use when any heat was applied to the tunnel.

Periodically during a run, the fuel tank cooling water temperature was read with a thermometer, and the cooling water exit temperature from the fuel probe read by thermocouple reading. These two never varied by more than a few degrees, so fuel injection temperature was assumed to be the average between the water tank and water exit temperatures.

RESULTS

General: The basic heat balance equation was used to obtain the percentage of fuel mass evaporated. The equation is as follows:

$$\dot{m}_a c_{p_a}(T_{a_1}-T_{a_2}) = \dot{m}_f H_v X + \dot{m}_f c_{p_f}(T_{a_2}-T_{f_1})X + \dot{m}_f(1-X)c_{p_f}(T_{f_2}-T_{f_1}) \quad \text{.....(4)}$$

The left side of the equation is the heat removed from the air to heat the fuel. The right side is first the heat of vaporization for the vaporized fraction, second, the heat to raise the vaporized fraction from its initial to its final temperature and lastly the heat to raise the liquid fuel droplets from their initial to equilibrium temperature. The manner of determining the various components in the heat balance equation is discussed in the next section of this report.

Thermocouple Error: In taking the data, it was found that the temperature drop measured in the spray at station 10 was always greater than that measured at station 18. This indicated a greater percentage of fuel vaporized at station 10 than at station 18, a physical impossibility. The two curves taken at the two separate stations seemed to remain parallel when plotted. However, at a low temperature or low fuel-air ratio, the data from station 10 indicated

a large temperature drop, decreasing with increasing fuel-air ratio or temperature, finally reaching a minimum and then increasing smoothly.

To investigate this phenomonon further, the thermocouple shown on the right in Fig. 11 was used to measure thermocouple spray shield temperature in the spray at stations 10 and 18. This thermocouple had a sensing element attached directly to the spray shield on the downstream side to measure shield temperature. It also had a sensing element behind the shield, but protected from the spray, to measure air temperature in the spray.

The dry air temperature before injection was read by both thermocouples and found equal. Fig. 19 shows the results of the survey at the two stations. From this it can be seen that the shield at station 10 is always cooler than the one at station 18.

Ref. 5, page 224, indicated the manner of calculating the true temperature of a gas. The heat balance equation for this relationship is as follows:

$$q_{gr} + q_c = q_r + q_k \qquad (5)$$

where q_{gr} is the rate of heat flow between the gas and thermocouple by gas radiation, q_c is the rate of heat flow between the gas and thermocouple by convection, q_r is the sum of the various terms representing the radiant heat interchange between the thermocouple and the various surfaces it "sees" and q_k is the heat conducted from the thermo-

couple to the walls confining the gas stream. Equation (5) can be written:

$$q_{gr} + h_c A_p(t_g - t_p) = h_r A_p(t_p - t_s) + q_k \qquad (6)$$

q_{gr} is negligible for the conditions being investigated. If q_k is also assumed negligible for the present, equation (6) reduces to

$$(t_g - t_p) = \frac{h_r(t_p - t_s)}{h_c} \qquad (7)$$

From equation (7) it can be seen that to reduce the thermocouple error $(t_g - t_p)$, the value of the numerator should be as small as possible and the value of the denominator as large as possible.

Fig. 20 shows how $(t_p - t_s)$ changes with inlet air temperature. From this figure it can be seen that the numerator of equation (7) goes to zero above 375 degrees Farenheit, indicating no error in the thermocouple readings due to radiation. Appendix I shows the method of calculating values for equation (7) for conditions when the radiation error is not zero. The radiation error can be shown to be negligible over most of the testing region.

Since the data taken for the variables of air temperature, air pressure, air velocity and fuel-air ratio does not show the curves for station 10 and 18 converging with increasing temperature or being properly displaced, that is with station 10 indicating less fuel vaporized than station 18 above 375^{o}F., the reason for the constant displacement of the two curves is conduction error.

As pointed out in Fig. 19, the shield surrounding the

temperature sensing element of the thermocouple at station 10 is always cooler by about 27°F than the shield surrounding the element at station 18. The shield is attached to the hypodermic needle tubing by piano wire and silver soldered. The thermocouple wire is led through the hypodermic needle tubing and although insulated electrically, its thermal insulation apparently is not too good. Thus heat is conducted from the thermocouple temperature sensing element to the cooler shield and hypodermic needle tubing.

Data was taken on the variables, air temperature, air pressure, air velocity and fuel-air ratio while the thermocouple error was being investigated. Originally it was suspected that liquid droplets were causing physical wetting of the temperature sensing element of the thermocouple, and attempts to build a better thermocouple were made. Since the slopes of the curves for the variables were what was desired, the conduction error did not invalidate the previously recorded data on the variables. This conduction error was used to advantage in obtaining the effect of axial length from the injector on fuel vaporization as will be shown later. Thermocouple error is further discussed in the next section.

Effect of Temperature on Fuel Vaporization: Fig. 21a shows the temperature drops measured at stations 10 and 18 in the fuel spray when inlet air temperature is varied and static pressure is held constant at 27 inches of mercury absolute, fuel-air ratio is held constant at .075, fuel

injection temperature is held constant at 74°F and air mass flow is held constant at 15.34 pounds per minute. To hold air mass flow constant, the velocity had to be varied to account for changing air density with temperature changes.

Fig. 21b shows the vaporization curves for the above conditions, calculated from equation (4) as shown in Appendix II. The dashed curve was obtained from Ref. 3, where iso-octane was the fuel injected at a constant pressure of 55 pounds per square inch, an air pressure of 25 inches of mercury absolute and an air velocity of 193 feet per second. Fuel was sprayed contrastream. Bahr, Ref. 3, made several runs at different air velocities and found all the curves to be quite similar but vertically displaced depending on what air velocity was used.

The benzene vaporization curves of Fig. 21b are similar to the iso-octane curve of Ref. 3, exhibiting good correlation. The degree of spray evaporation related to the experimental variable temperature is found by plotting the benzene evaporation curves on a log-log plot. A plot of temperature versus percent fuel vaporized does not produce a straight line on a log-log plot, but if the function $\frac{N}{100-N}$ is used, the curve can be closely approximated by a straight line. By this method then

$$\frac{N}{100-N} = K(T_a)^{4.00} \qquad (8)$$

where K is an adjusting constant and T_a is in degrees Rankine.

Effect of Static Pressure on Fuel Vaporization: Fig. 22a shows the temperature drops measured in the fuel spray when static air pressure was varied while inlet air temperature was held constant at 325°F, fuel-air ratio was .075, fuel injection temperature was 75°F and air mass flow was 15.34 pounds per minute.

Fig. 22b shows the vaporization curves calculated from the temperature drops. The dashed curve is from Ref. 3, taken under the following conditions: Air temperature, 319°F; air velocity, 199 feet per second; fuel, iso-octane injected at 55 pounds per square inch pressure.

When the benzene data was taken, an apparent discontinuity was found in the curves. The first run was made with air pressure starting high and decreasing. To check the data, another run was made starting with low air pressure and increasing it. Nothing else was changed in the manner of obtaining the data. Again an apparent discontinuity was found in the curves. The discontinuity occurs at a pressure of 26 inches of mercury absolute. Since all the variables are held constant except static air pressure, the discontinuity in the curves can only be caused by an instrumentation error, specifically an error in indicated temperature drop in the spray. Somehow, around 26 inches of mercury absolute the conduction error changes appreciably. Since the curves are all similar to the NACA curve, the phenomonon was not investigated further, being a side issue.

The non-similarity of the vaporization curve from sta-

tion 10 below 24 inches of mercury absolute is attributed to thermocouple conduction error.

The degree of vaporization due to inlet air pressure was found from a log-log plot to be

$$\frac{N}{100-N} = K(P_a)^{-0.84} \qquad (9)$$

where K is an adjusting constant not the same as the constant for the temperature function, and P_a is in inches of mercury absolute.

Effect of Velocity on Fuel Vaporization: Fig. 23a shows the data obtained when inlet air velocity is a variable. The constant conditions for the other variables were: Temperature, 190°F; air pressure, 27 inches of mercury absolute; fuel injection temperature, 75°F; and fuel-air ratio, .022.

Fig. 23b shows the velocity effect on percentage of fuel evaporated. Only one curve is shown, that taken from data at station 18. The data from station 10 showed a strong thermocouple error below a velocity of about 100 feet per second. When calculated, this data gave results indicating over 100 percent fuel vaporization, which could not be used in the function $\frac{N}{100-N}$.

The data points on the one evaporation curve are admitedly rough, but for a reason. With a low fuel-air ratio, the maximum temperature drop for 100 percent vaporization is low and each degree of error in obtaining the temperature in the spray has more significance. When the temperature drop is converted to percent evaporated, the error is

magnified.

The dashed line in Fig. 23b shows the effect velocity has on contrastream injection of iso-octane under approximately similar conditions as taken from Ref. 3. No correlation was expected in this case because evaporation with contrastream injection would tend to be better, since increasing inlet air velocity increases the degree of atomization of the injected fuel spray.

From a log-log plot of velocity and percent of fuel evaporated, the degree of evaporation due to varying inlet air velocity was found to be

$$\frac{N}{100-N} = K(V_a)^{-1.43} \qquad (10)$$

where K is again an adjusting constant different from others previously mentioned and V_a is in feet per second.

Effect of Fuel-Air Ratio on Vaporization: Fig. 24a shows the temperature drops obtained in a benzene spray when the fuel-air ratio was varied and inlet air temperature held at 325°F, air pressure 27 inches of mercury absolute, inlet air velocity 50 feet per second, and fuel injection temperature 71°F.

Fig. 24b shows the results of the data when percent of fuel evaporated is calculated. The curve of data for station 10 is erroneous due to a strong conduction error in the thermocouple below a fuel-air ratio of .06. The data from station 18 appears to be good throughout the investigated range of the variable.

From a log-log plot of fuel-air ratio and percent of

fuel evaporated, the degree of evaporation due to fuel-air ratio was found to be

$$\frac{N}{100-N} = K(F/A)^{-0.27} \qquad (11)$$

where K is a new adjusting constant and fuel-air ratio is dimensionless.

Effect of Axial Length From the Nozzle on Vaporization: To arrive at an answer to the effect on vaporization of axial length, the spray shield data obtained in Fig. 19 in determining the nature of the thermocouple error was used.

The average temperature difference between the curves at stations 10 and 18 for the variables air temperature, air pressure, inlet air velocity and fuel-air ratio was found to be 13.9°F. But at an air temperature of 300°F, fuel-air ratio of .075, an inlet fuel temperature of 76°F and an air pressure of 27 inches of mercury absolute, Fig. 19 shows the difference between the shield temperatures at stations 10 and 18 to be 27°F, the shield at station 10 being 27°F cooler than that at station 18. Since the average temperature difference in the experimental curves is only 13.9 degrees, obviously all the conduction cooling effect is not being applied.

Now, if it is assumed that the thermocouple at station 18 reads correctly and all the differential conduction cooling of 27°F is error in the thermocouple at station 10, then the curve of data from station 10 would be 13.1 degrees below the curve of data from station 18. This is the greatest displacement the two curves could have and calculations

of the effect of axial length on fuel vaporization made from this assumption would give the largest effect possible.

Solving the heat balance equation, equation (4), with an assumed inlet air temperature of 300°F, fuel-air ratio .075, a fuel injection temperature of 76°F and a ΔT of 13.1°F gives 14.1 percent increase in fuel vaporized between stations 10 and 18.

Fig. 25 shows an assumed effect of axial length on percent of fuel vaporized with the above assumptions. The curve starts at zero and has an increase of 14.1 percent in 7.85 inches, the distance between the two thermocouples at stations 10 and 18.

A log-log plot of this curve shows the maximum effect of axial length on fuel vaporization to be

$$\left[\frac{N}{100-N}\right]_{max} = (L)^{1.23} \qquad (12)$$

where L is in inches. The true effect is certainly less than this, but obtaining a solution in the above manner gives an order of magnitude of the effect of axial length as compared to the other variables investigated.

DISCUSSION

The air flow through the test section is assumed to be one dimensional, steady and isentropic except in the boundary layer next to the walls. Fig. 17 shows the flow through the test section to be reasonably uniform.

In using equation (4), the heat balance equation, in calculating the percent of fuel vaporized it is assumed that:

a. The average value of the specific heats, c_p, for the fuel and air may be used over the entire range of temperatures.

b. The air temperature in the fuel spray is accurately known from measurement.

c. Equilibrium conditions have been attained in the spray, that is, the fuel droplets have reached their wet bulb temperature before reaching the thermocouples.

d. The difference between the liquid and surface temperature of any fuel droplet is negligible.

e. The fuel injection temperature is accurately known.

f. No heat loss occurs through the walls of the tunnel, and the flow is isentropic.

g. The fuel-air ratio is accurately known.

All values in equation (4), the heat balance equation, are known by measurement except the temperature to which the fuel droplets are heated in the tunnel. El Wakil in Ref. 6 confirmed the theory of infinite thermal conductivity in a fuel droplet, and was able to photograph the circulation in a droplet. This permits assuming the droplet surface temperature is equal to the liquid interior temperature.

Ingebo in Ref. 2 gives curves of wet bulb temperature for different fuels at various air temperatures and Fig. 26 is derived from his data. By entering Fig. 26 with the dry air temperature, the wet bulb or equilibrium temperature of the fuel droplet is found for use in equation (4).

Since the amount of heat taken from the air to heat the fuel droplets to their wet bulb temperature is small compared to the heat used to vaporize the fuel fraction in this work, and the effect of pressure on wet bulb temperature is small anyway, pressure effect on wet bulb temperature is ignored.

A problem to be reckoned with in fuel sprays is wetting of the chamber or tunnel walls by the fuel. In a jet engine it causes coking and in a wind tunnel it upsets the calculation of the fuel-air ratio in the tunnel. The fuel-air ratio is very rich next to the walls of the tunnel where film evaporation is taking place along with spray vaporization. When this happens in a tunnel, the overall fuel-air ratio is not representative of the fuel-air ratio in

the area away from the tunnel walls.

To combat this problem, an attempt to build a variable area, narrow cone, injection nozzle was made. Fig. 27 shows this nozzle in the middle of the three shown. The nozzle was a pintle type Diesel nozzle taken from a Bosch injector and modified with a brass adaptor to fit the plumbing in the wind tunnel. The pintle was attached to an internal screw arrangement which could be turned to adjust the fuel flow rate. Two problems plagued the work with this nozzle. First the orifice was so small, a minute particle of dirt in the fuel could plug it. But the real problem was in not being able to get a high enough fuel pressure to properly atomize the fuel.

A second attempt was made to combat the wall wetting problem by building a nozzle as shown on the left in Fig. 27. This nozzle had a hollow brass body with three spikes screwed in at 120 degree intervals. The spikes were drilled almost to the outer tip, where the injector orifice was drilled in. The orifice in each spike was made with a number 78 drill having a diameter of .016 inches. To make the fuel atomize better, "V" slots were cut into each orifice with a jeweler's file. These produced better atomization of the fuel.

Injection was tried spraying downstream and contrastream with the latter producing better results. A satisfactory pattern could not be achieved spraying downstream. With contrastream spraying, atomization was very good, but

large liquid drops tended to fall from the lowest part of the nozzle main body from leaks at the spike threads, upsetting temperature measurements in the test section. This nozzle also had a tendency to plug with dirt at the slightest provocation, necessitating the unbolting of the test section to get at it for cleaning.

So, for reliability, a uniform spray pattern, proper atomization and in the interests of getting on with the experimenting, the Hago atomizing nozzle shown in Fig. 27 on the right was installed and gave satisfactory operation for the remainder of the work.

The fuel-air ratio was chosen to be .075 because this is approximately stoichiometric for benzene and air. With a large fuel-air ratio, a large temperature drop in the spray is possible making the accuracy of the work better. Benzene was used because it was available, has a large heat of vaporization and is a pure hydrocarbon.

Maintaining a high air inlet temperature in the tunnel also made possible a large temperature drop in the spray since more fuel was vaporized, making for better accuracy of results. For this reason, when air temperature was being held constant, it was made as high as practicable.

The fuel-air ratio was made a parameter instead of fuel injection pressure to simplify operating the tunnel and calculation of the percent of fuel vaporized. The fuel pressure and flow were not easily adjusted, so if it could be done once and left alone, operating was simplified. Since

the fuel injection rate was to be held constant and it was desired that fuel-air ratio be held constant, then air velocity had to be adjusted to keep the air mass flow constant with changing air pressure and temperature. The air velocity was easily adjusted by turning the inlet air valve until the proper dynamic pressure was read on the inclined tube manometer. The method was very accurate.

In the early stages of testing, before the Hago nozzle was installed, traverses of the tunnel were made with the thermocouples before and during injection. This was done to obtain the average percentage of fuel vaporized at each station and was necessary because the spray pattern was not uniform and the temperature profile was not flat. It also was not similar with different heater combinations. The results with this method left a great deal to be desired.

With the Hago nozzle, the spray pattern was uniform throughout, being designed this way. By analyzing the temperature profiles, Fig. 18, a point 1.45 inches from the tunnel wall at stations 10 and 18 was found to be representative of the average temperature at the stations. This then permitted placing the thermocouples 1.45 inches from the wall and the readings would be the average at the station. The savings in fuel, time and effort were enormous using this method. And the accuracy of the results improved considerably!

Three separate factors enter into the determination of the actual fuel-air ratio in the test section. The con-

duction error may be thought of in two parts, first, a cooling of both thermocouple elements by a constant amount, and second, a differential cooling of the thermocouples due to one being closer to the nozzle than the other. The conduction error causes a larger temperature drop to be read by the thermocouple in the spray than is correct. When this temperature drop is converted to percent of fuel vaporized, this percent is greater than the true value which would be determined from a true reading of the temperature drop in the spray. The true fuel-air ratio in the area around the thermocouples is the third part of the problem. This is something less than the overall fuel-air ratio through the tunnel due to the wetting of the tunnel walls by the conical spray from the nozzle. To off-set the indication of a larger than true percent of fuel vaporized, the overall fuel-air ratio is used in the calculations.

Conduction error tends to displace the vaporization curve vertically upward on the percent vaporized ordinate, while using the overall fuel-air ratio tends to displace the vaporization curve downward on the same ordinate. The two errors, conduction and fuel-air ratio, do not cancel each other but tend to minimize each other in the calculations. For this reason, the character of the curves is true but the actual percentage vaporized is only a relative number.

The reason for the thermocouple shield at station 10 being cooler than the shield at station 18 is explained by

the fact that from visual observation of the two shields, the one at station 10 intercepts more droplets than station 18. In other words, there is more liquid evaporating off the hot shield at station 10 than at station 18. The number of droplets decreases with axial length due to the vaporization process.

The percentage error in the calculated percent of fuel vaporized decreases with larger possible total temperature drops for one hundred percent vaporization. For this reason, fuels with high heats of vaporization, at high fuel-air ratios and at high temperatures should be utilized. Measuring the amount of fuel vaporized by measuring temperature drop in a spray then has limited application, due to the aforementioned considerations.

Good correlation with the work of NACA as done by Bahr in Ref. 3 was obtained on the parameters of inlet air temperature and pressure, indicating these two variables are not affected by contrastream or downstream injection of the fuel.

Air inlet velocity causes more atomization in contrastream injection than in downstream injection. Therefore, no correlation could be expected with these two methods of injection. In downstream injection, the droplets are probably not accelerated too rapidly by a fast inlet air flow, so with increasing air inlet velocity the vaporization rate would be expected to decrease.

The computation of the effect of axial distance from

the injector is admittedly only a rough approximation. The calculations were made only to approximate the extremes of the operating envelope for this effect. And it can safely be stated that the inlet air temperature has a much greater effect on the amount of fuel vaporized than does axial length. But by the method, the axial distance effect is placed somewhere near its relative position with the other parameters.

The discrepancy between the exponents determined for the parameters of inlet air temperature and pressure in this work and the NACA work of Ref. 3 is due to the NACA values being an average of curves determined from several inlet air velocities. When a curve depicting conditions which were similar to those of this work was chosen, the correlation was very good, as seen in Figs. 21 and 22.

CONCLUSIONS AND RECOMMENDATIONS

1. The effect of inlet air temperature has the strongest influence on the amount of benzene fuel vaporized. With increasing temperature, an increasing amount of fuel is vaporized. The effect may be shown by the function

$$\frac{N}{100-N} = K(T_a)^{4.00} \tag{8}$$

2. With increasing inlet air pressure, the amount of benzene fuel vaporized decreases. This effect may be depicted by the function

$$\frac{N}{100-N} = K(P_a)^{-0.84} \tag{9}$$

3. With increasing air inlet velocity, the amount of benzene fuel vaporized decreases. The influence may be approximated by

$$\frac{N}{100-N} = K(V_a)^{-1.43} \tag{10}$$

4. The percent of fuel vaporized with increasing overall fuel-air ratio decreases. The effect is slight however, and may be shown by

$$\frac{N}{100-N} = K(F/A)^{-0.27} \tag{11}$$

5. The effect of axial distance from the fuel injector is to increase the percent of fuel vaporized with increasing distance. The maximum effect of this parameter is shown by

$$\left[\frac{N}{100-N}\right]_{max} = (L)^{1.23} \tag{12}$$

6. The technique of determining percent of fuel vaporized by measuring the temperature drop in a fuel spray is best used when the temperature drop possible for 100 percent vaporization is large.

7. Shielded thermocouples for use in spray temperature measurement should be constructed of heat insulated materials to minimize or eliminate the conduction error caused by a cool shield taking heat from the temperature sensing element of the thermocouple.

8. Conduction and fuel-air ratio errors merely displace the vaporization curve on the percent vaporized ordinate, and do not affect the slope of the curves in the range investigated in this work.

9. Further work in fuel vaporization with the present equipment if attempted, should be with some form of probe equipment which would permit the actual measurement of the fuel-air ratio in a spray. The NACA Analyzer of Ref. 3 is an example of this method.

REFERENCES

1. El Wakil, M.M. et al, "Theoretical Investigation of the Heating Up Period of Injected Fuel Droplets Vaporizing in Air." NACA Technical Note 3179, May 1954.

2. Ingebo, R.D., "Vaporization Rates and Heat Transfer Coefficients for Pure Liquid Drops." NACA Technical Note 2368, July 1951.

3. Bahr, D.W. "Evaporation and Spreading of Iso-octane Sprays in High Velocity Air Streams." NACA Research Memorandum E 53I14.

4. Foster, H.H. and Ingebo, R.D. "Evaporation of JP-5 Fuel Sprays in Air Streams." NACA Research Memorandum E 55K02.

5. McAdams, W.H. "Heat Transmission" 2nd edition. McGraw Hill Book Co. Inc.

6. El Wakil, M.M. et al, "Experimental and Calculated Temperature and Mass Histories of Vaporizing Fuel Drops" NACA Technical Note 3490, January 1956.

FIG 1

TEST SECTION

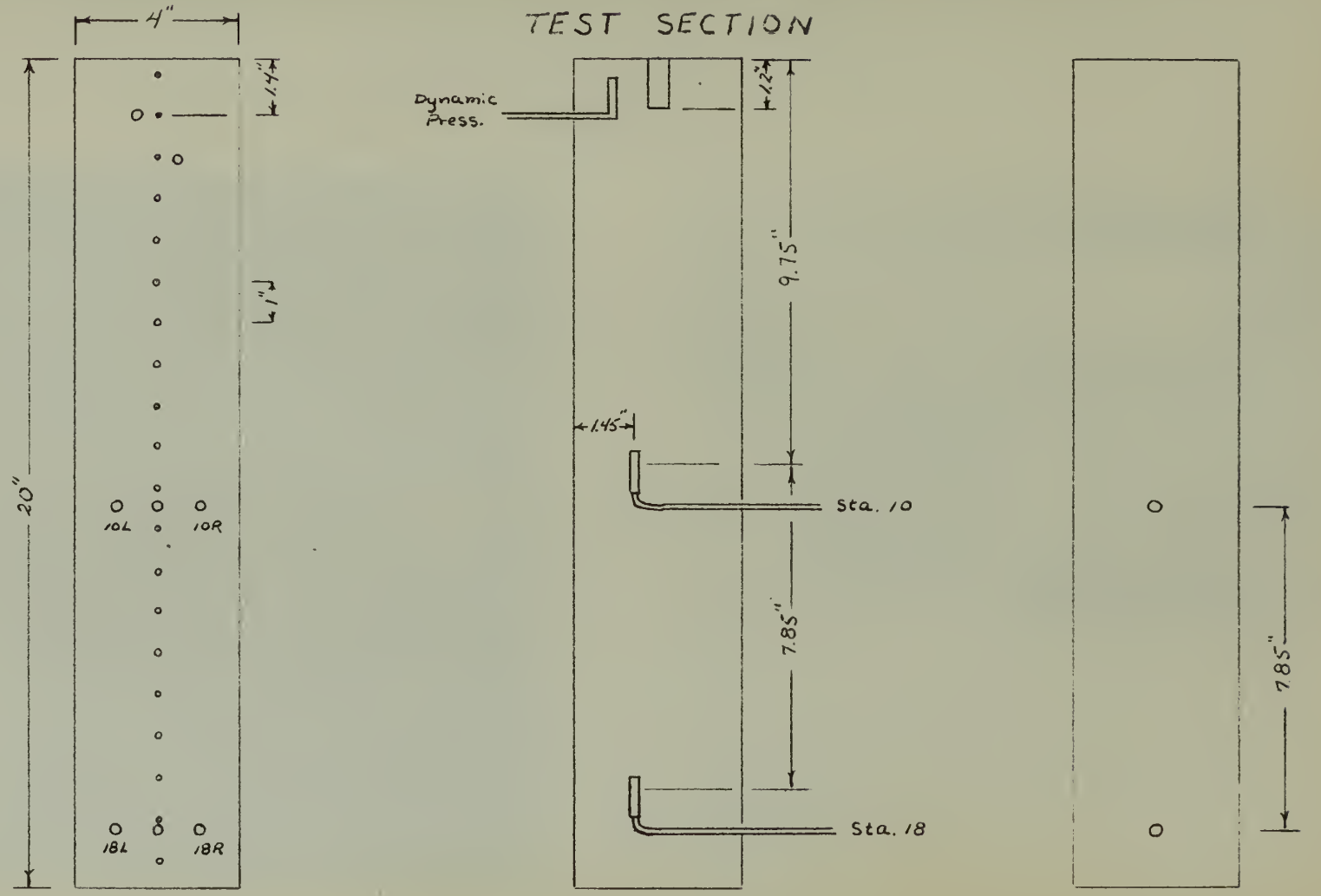

LEFT FACE

OPERATOR'S VIEW

RIGHT FACE

Fig. 3

Hago Atomizing Nozzle
150 psig.

FIG 4

GENERAL TUNNEL LAYOUT

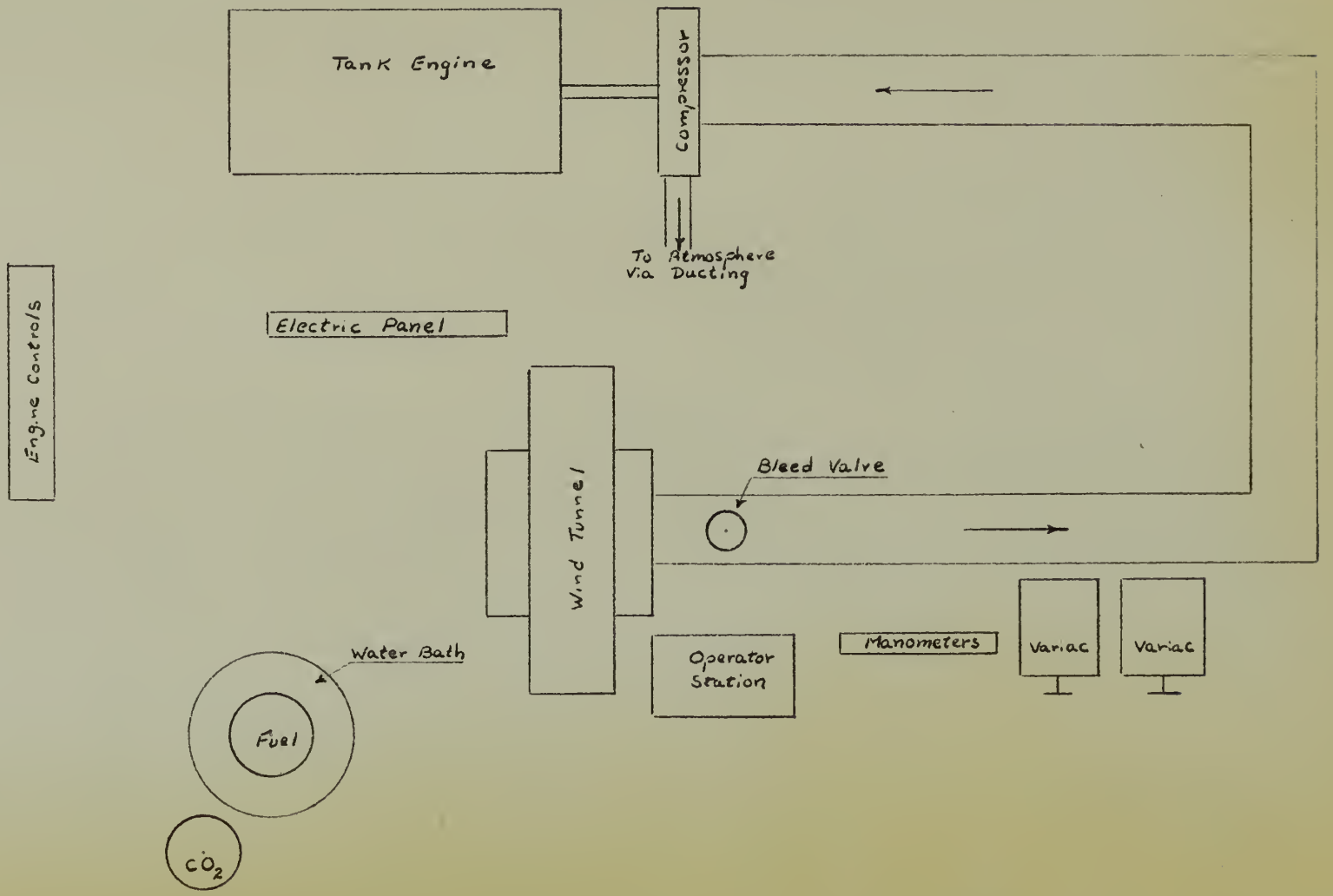

FIG 5

TUNNEL ELEVATION

(viewed from operator's station)

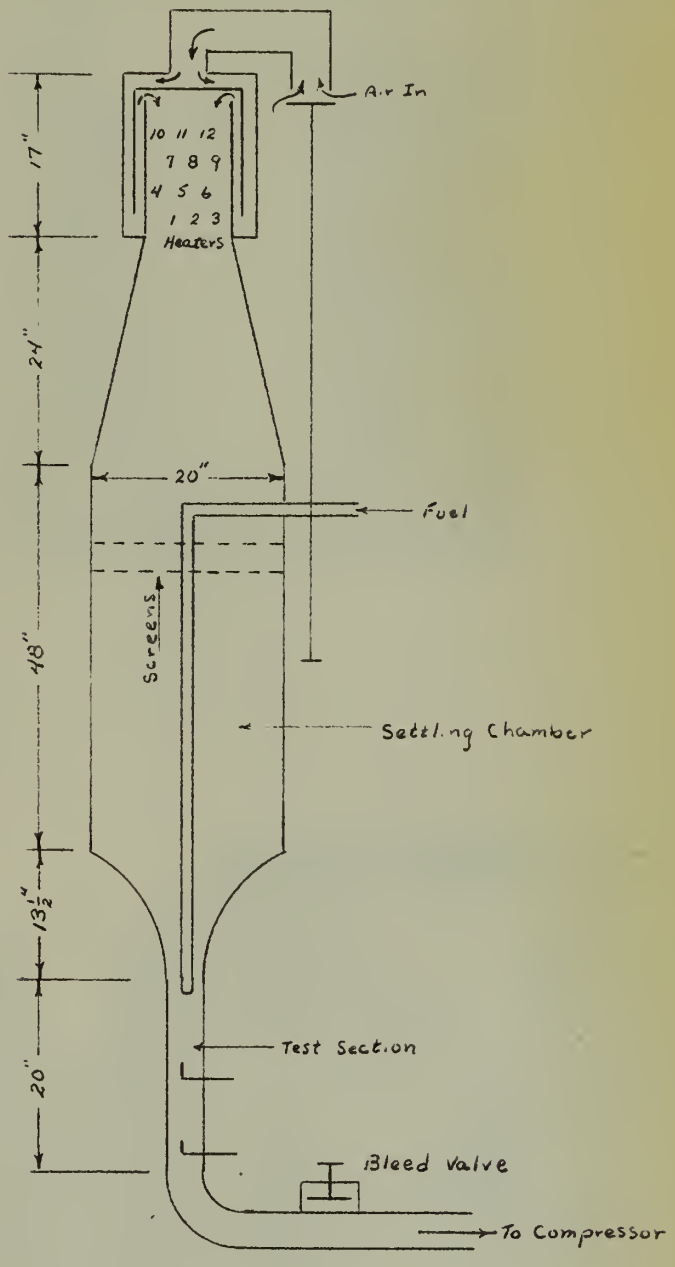

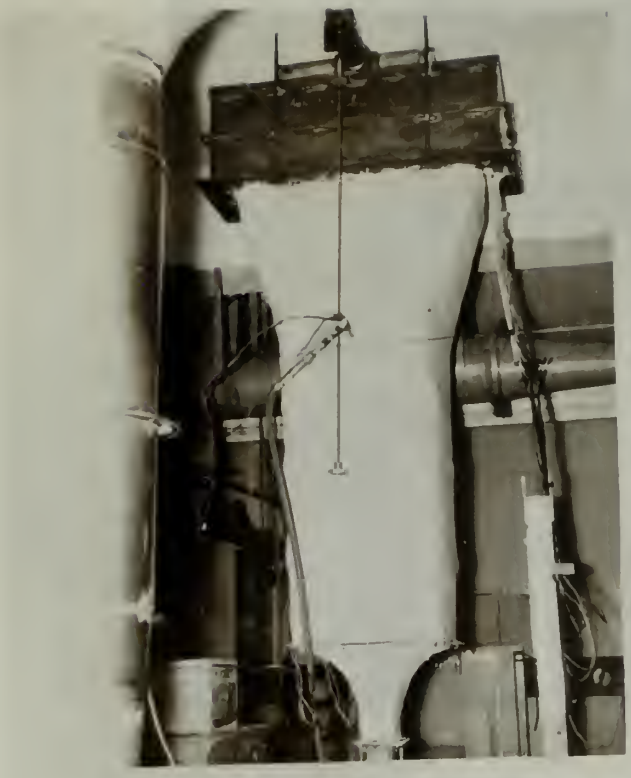

Fig. 6

Wind Tunnel

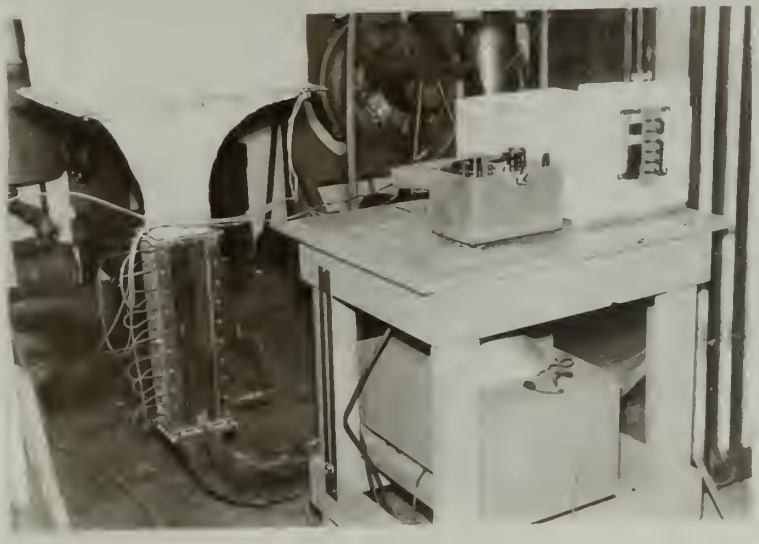

Fig. 7

Test Section and Operator's Station

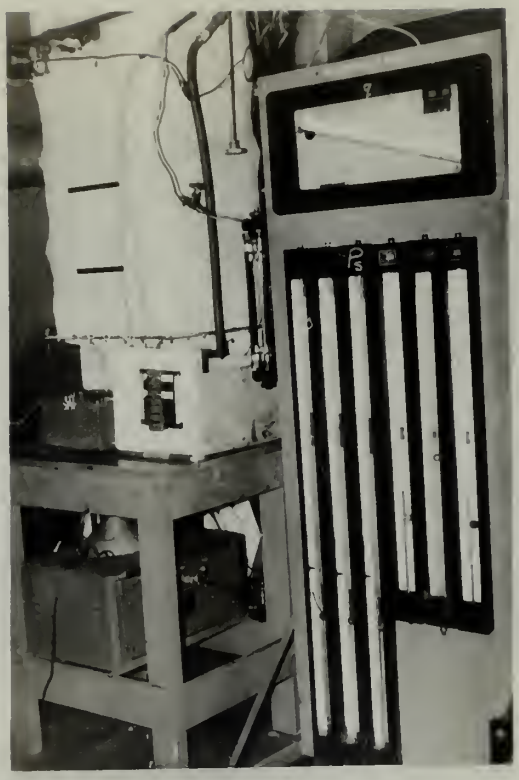

Fig. 8

Manometer Board

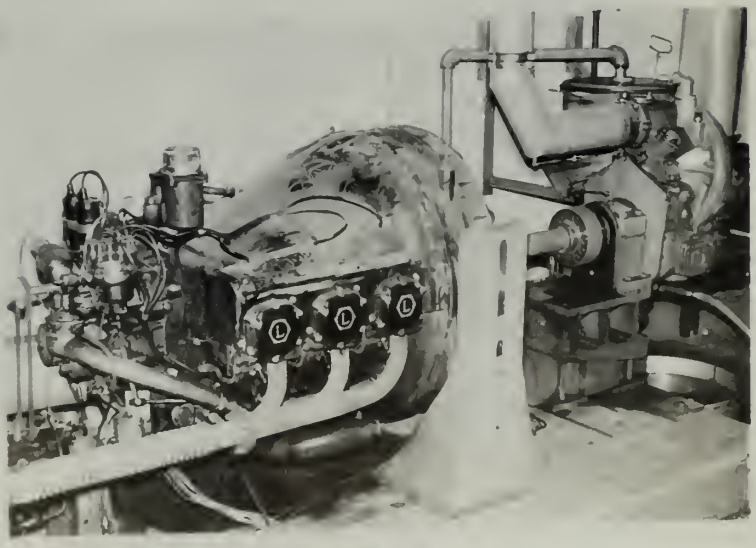

Fig. 9

Lycoming Test Engine
and Centrifugal Dynamometer

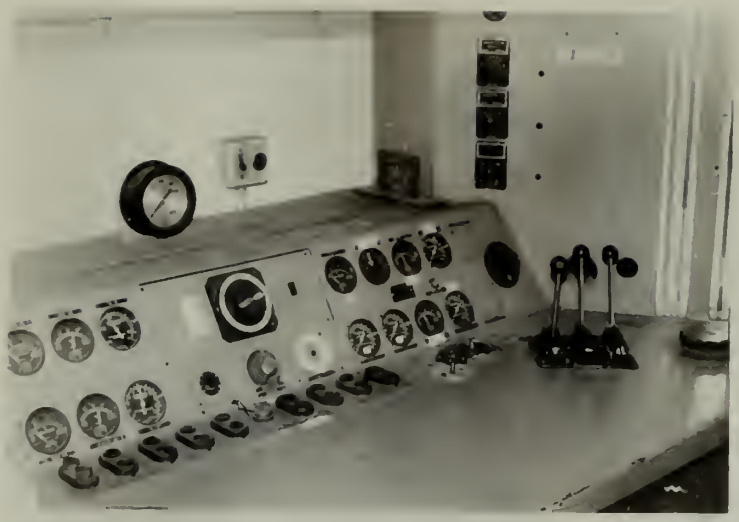

Fig. 10

Engine Control Panel

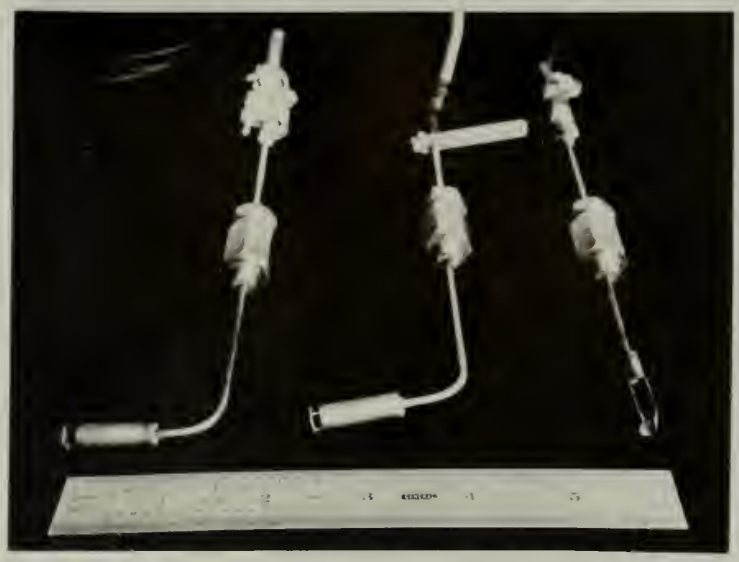

Fig. 11

Shielded Thermocouples

FIG 12
THERMOCOUPLE DETAIL

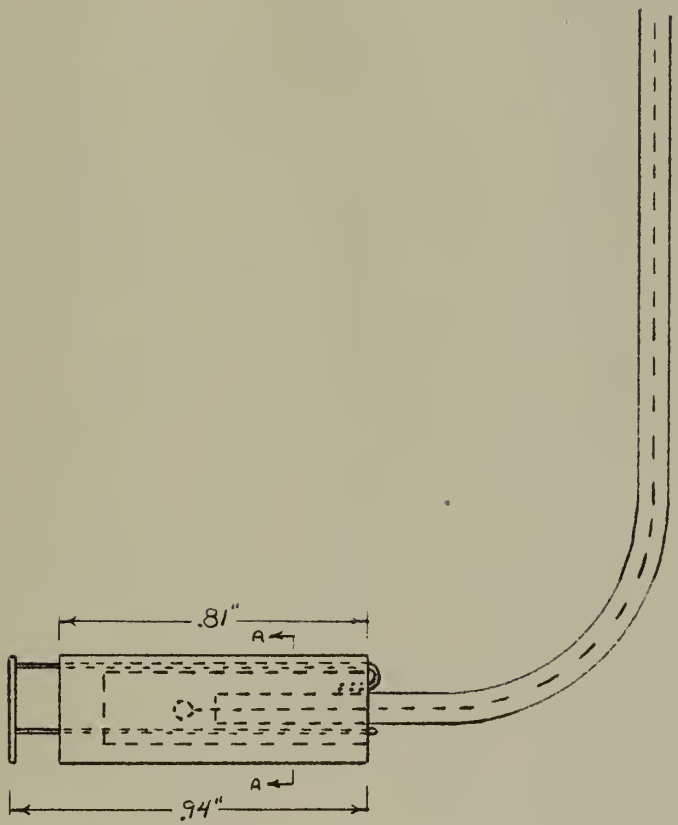

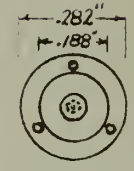

Section A-A

FIG 13

TUNNEL OPERATING NOMOGRAPH TO DETERMINE DENSITY

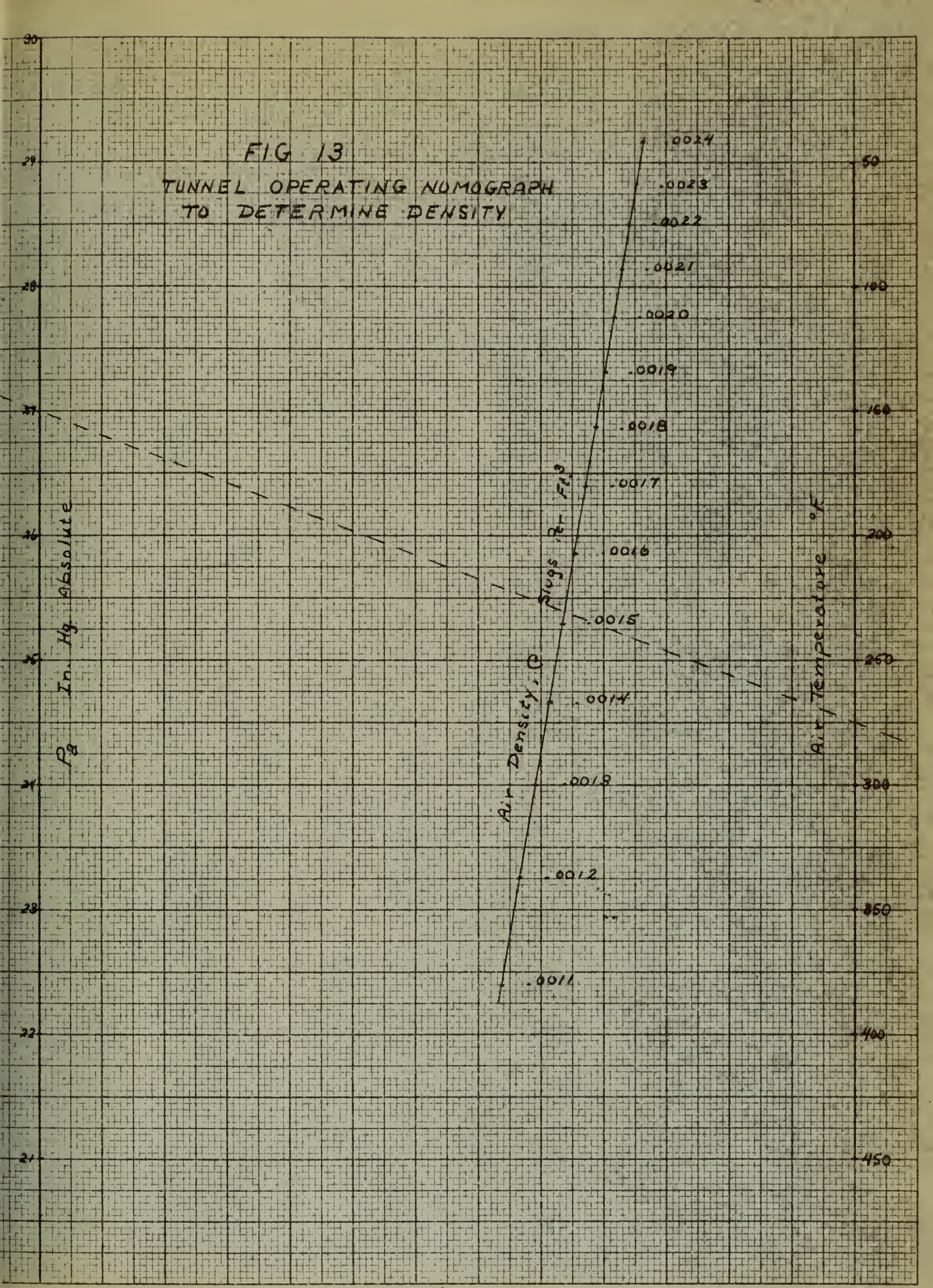

FIG 14

TUNNEL OPERATING NOMOGRAPH TO DETERMINE h OR V_a

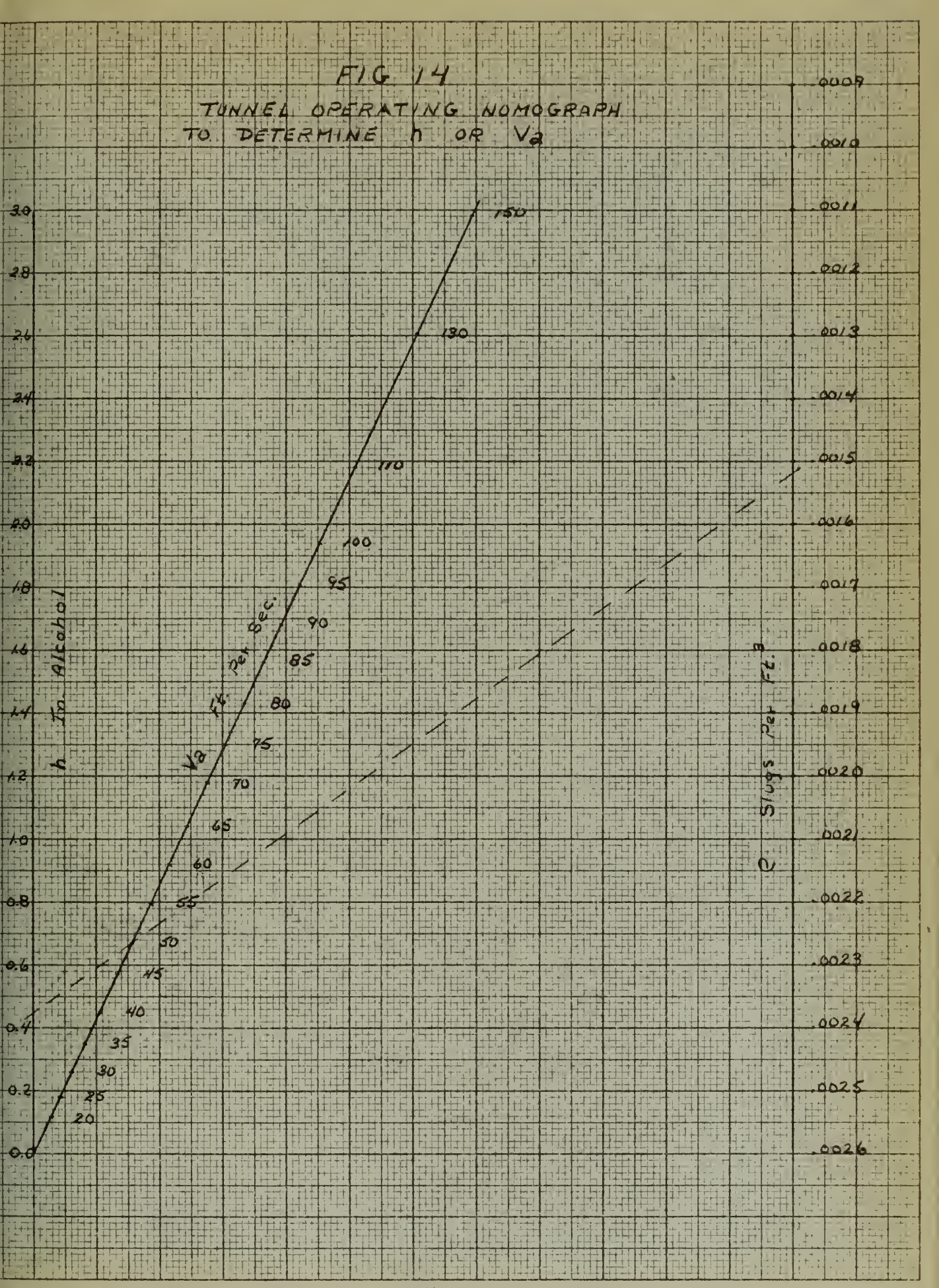

FIG 15

HAGO NOZZLE CALIBRATION

(Atmospheric Press 27" Hg Abs)

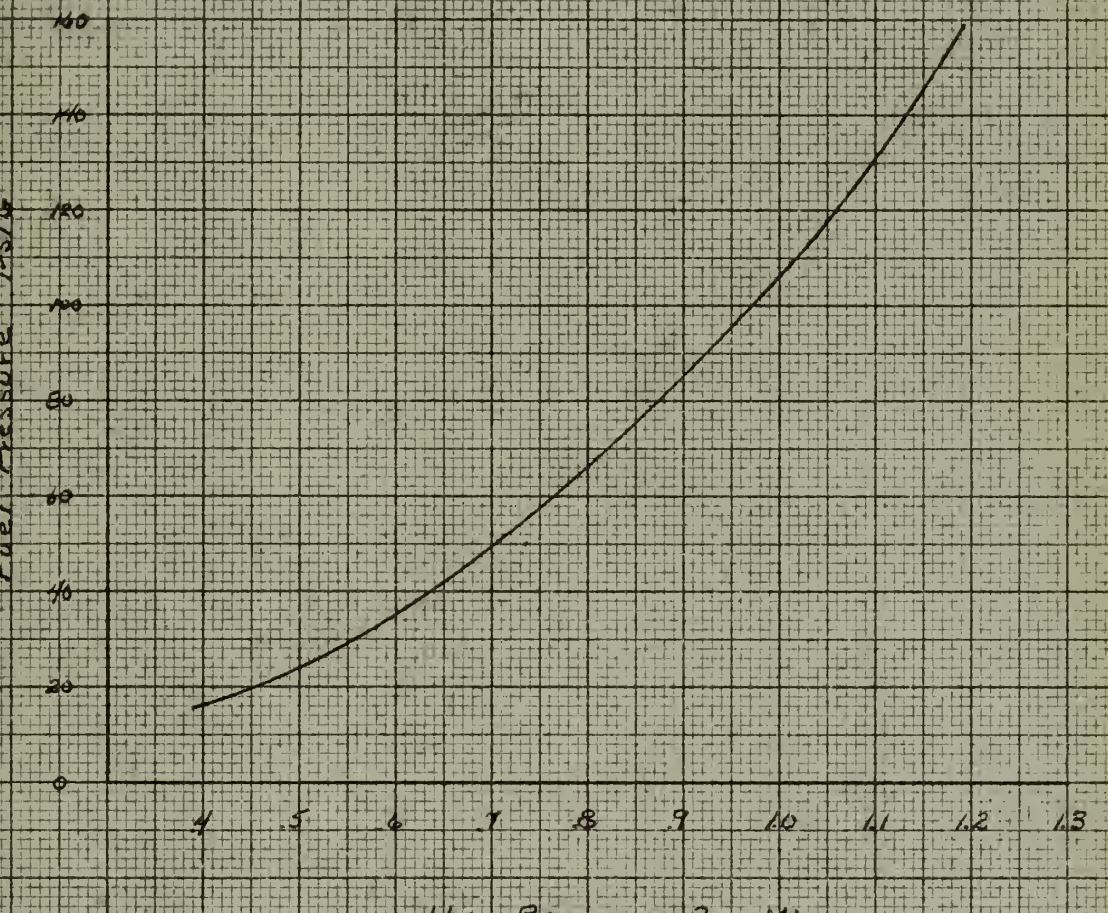

FIG 16

FUEL FLOW METER
CALIBRATION FOR BENZENE

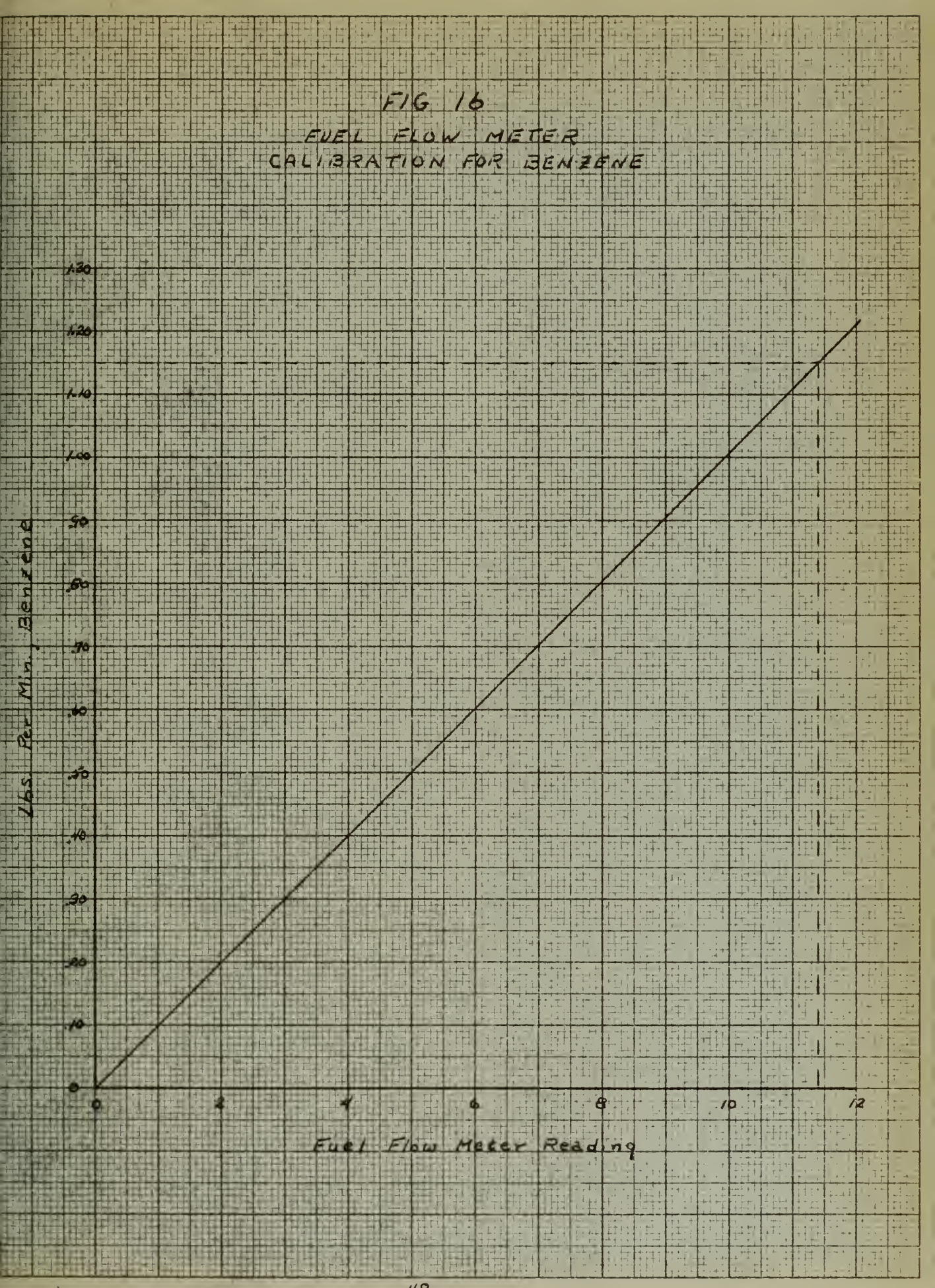

FIG 17

AIR VELOCITY PROFILES

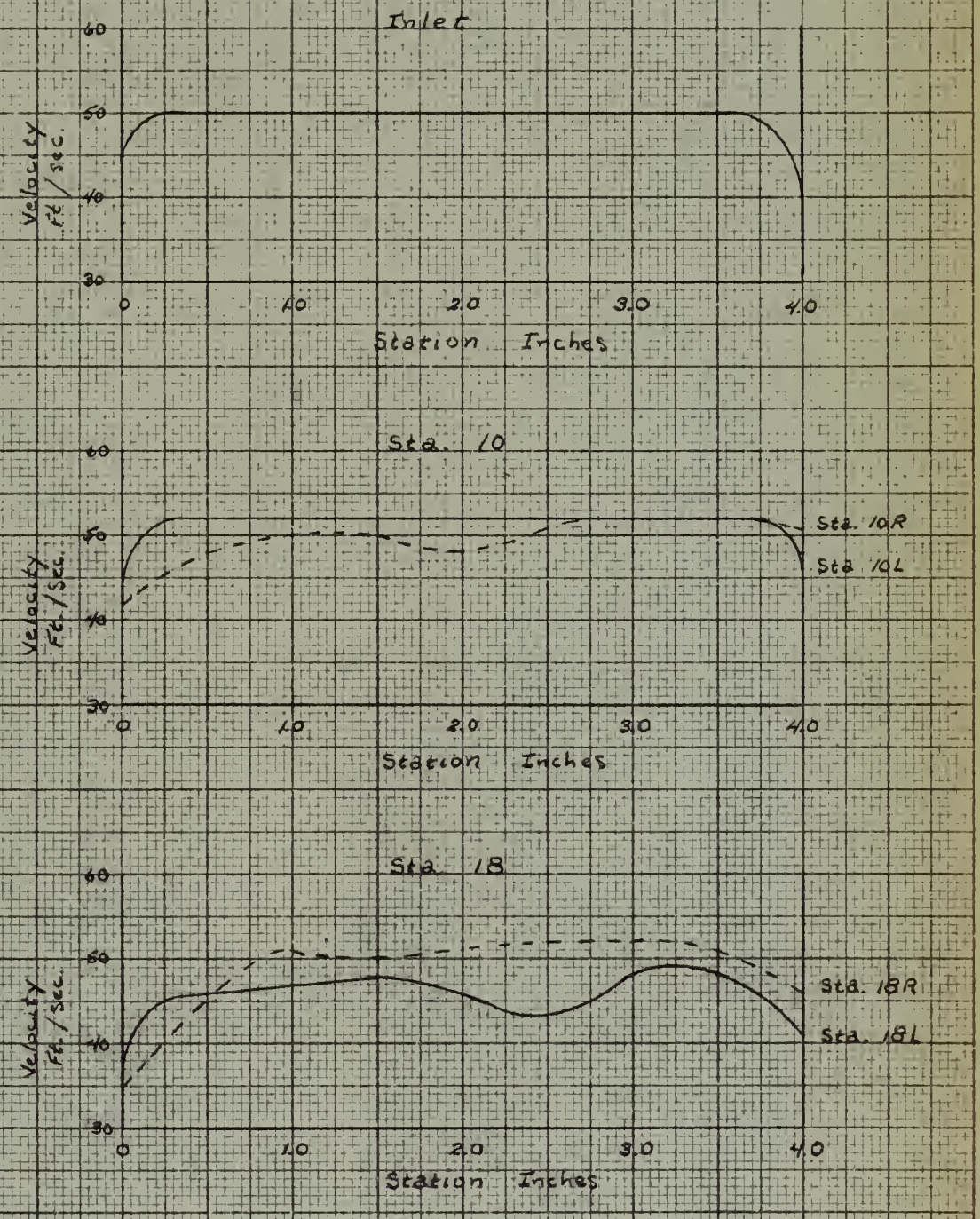

FIG 18

AIR TEMPERATURE PROFILES

Velocity = 50 Ft/Sec P_2 = 27 In Hg

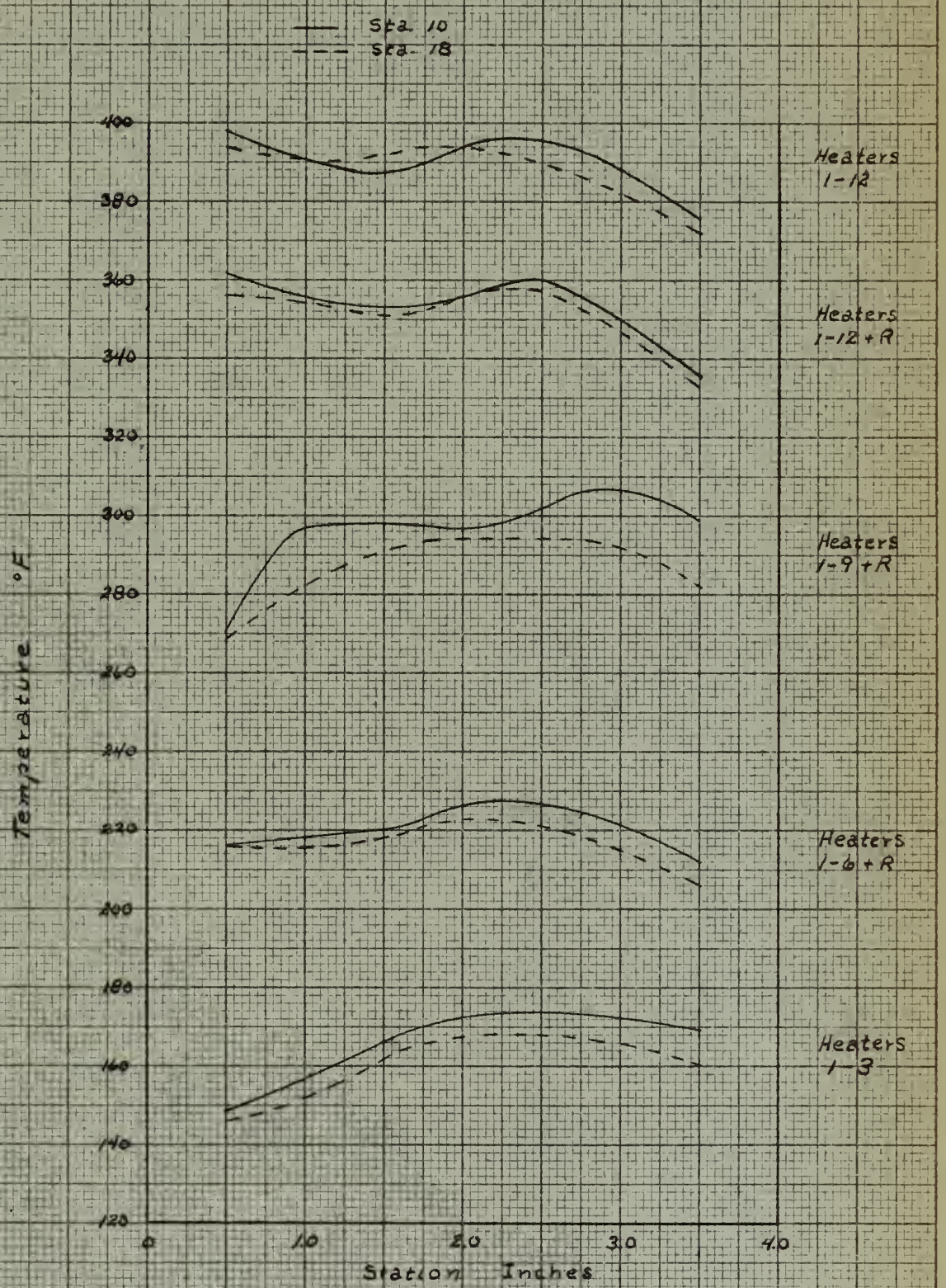

FIG 19

THERMOCOUPLE SHIELD TEMPERATURE

F/A = .075 P_a = 27 In. Hg.

T_a = 76°F V_a approximately 50 Ft/Sec.

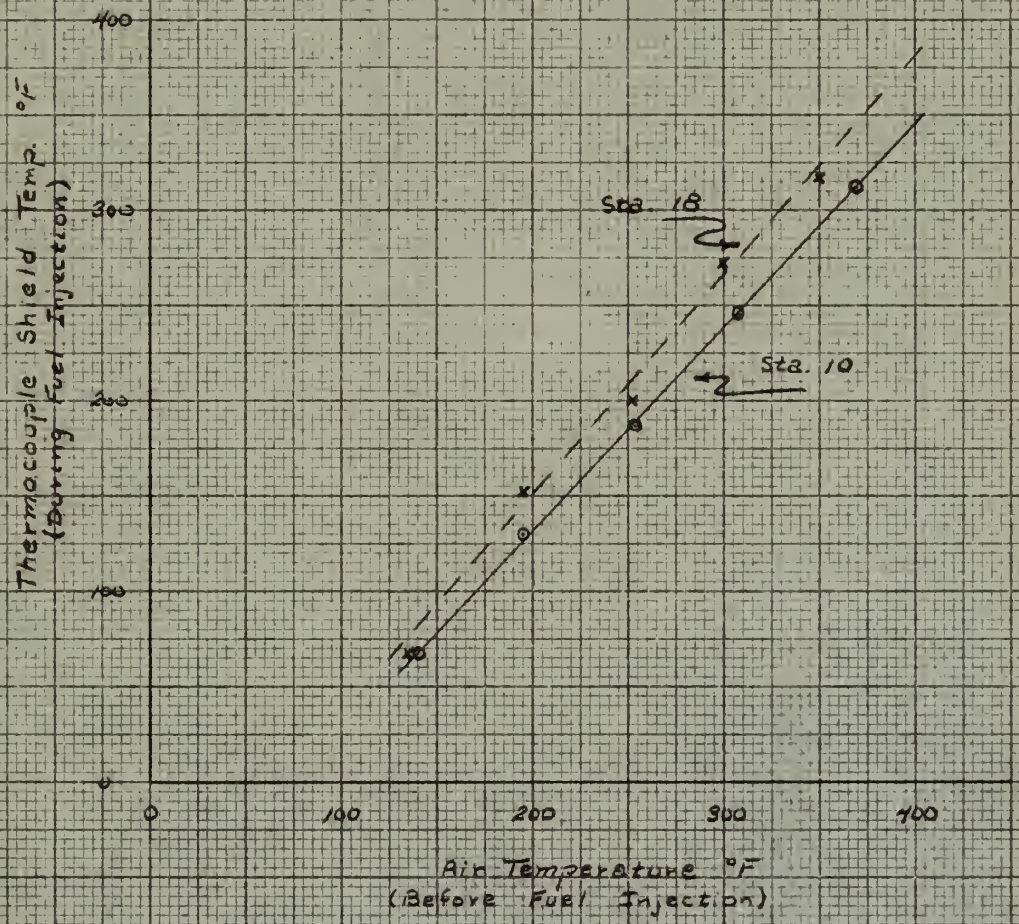

FIG 20

TEMPERATURE DIFFERENCE BETWEEN THERMOCOUPLE AND SHIELD

F/A = .075 P_a = 27 In. Hg.

T_i = 76°F V_2 approximately 50 Ft/Sec.

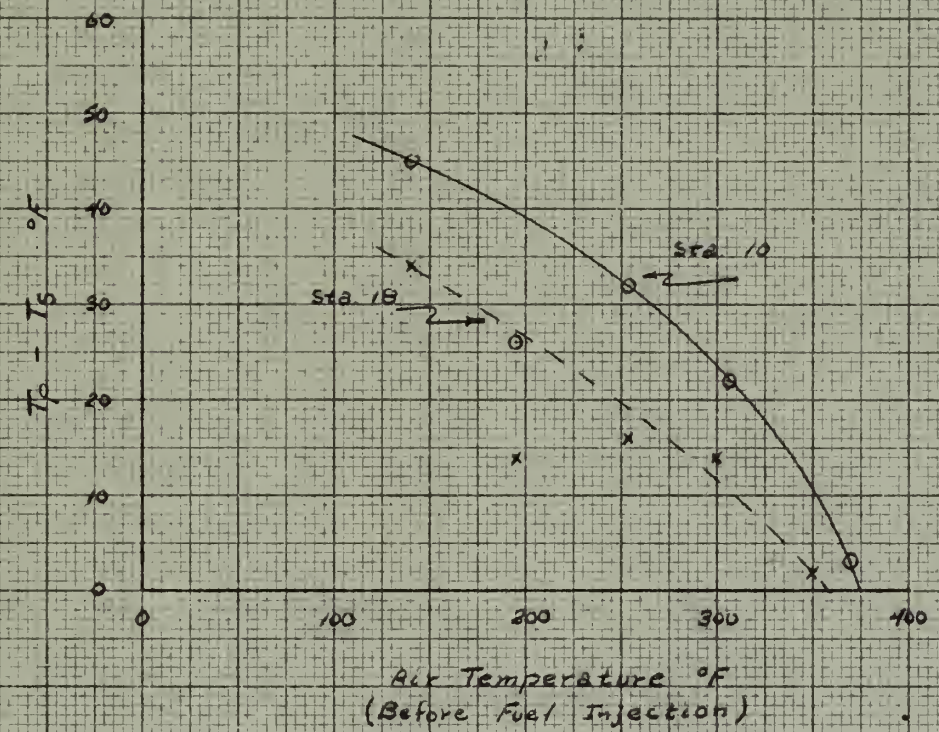

FIG 21a

INLET AIR TEMPERATURE INFLUENCE

P_2 = 27 In. Hg V_2 = 43-55 Ft./Sec.

F/A = .075 T_f = 74° F

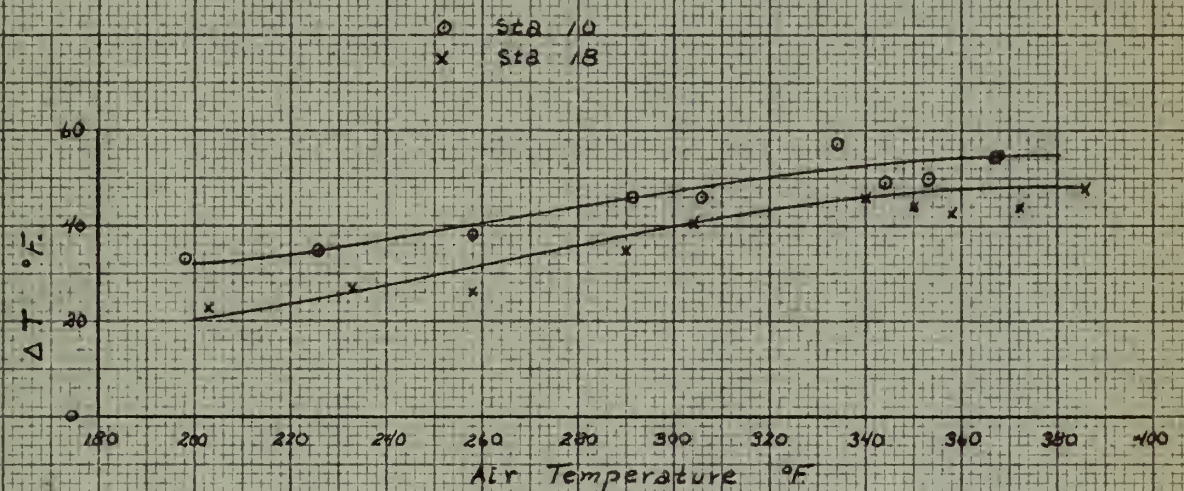

FIG 21b

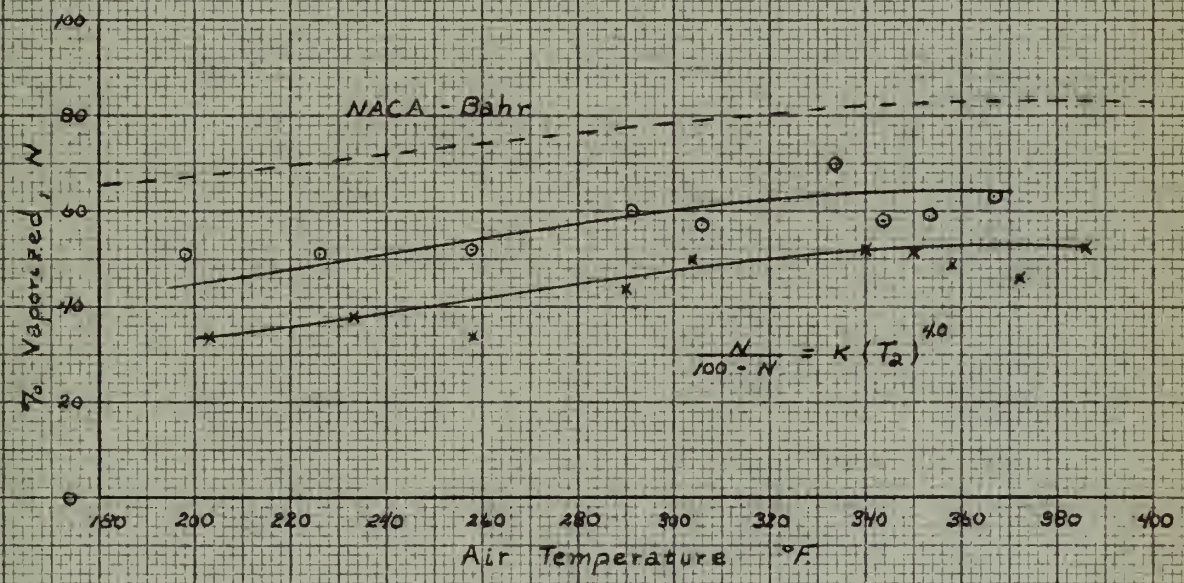

FIG 22a

STATIC AIR PRESSURE INFLUENCE

T_{a_1} = 325°F V_2 = 49-63 Ft./Sec.

F/A = .075 T_{f_1} = 75°F

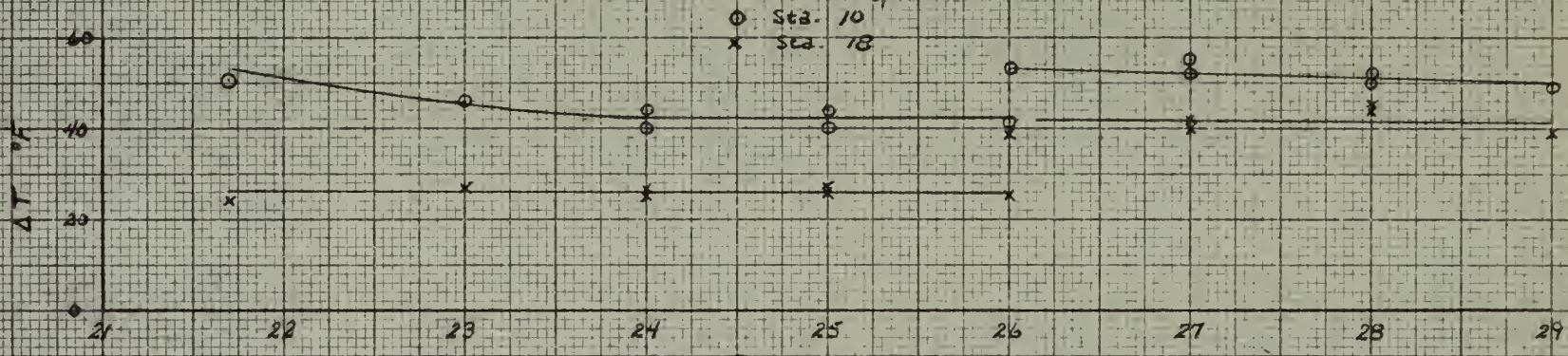

FIG 22b

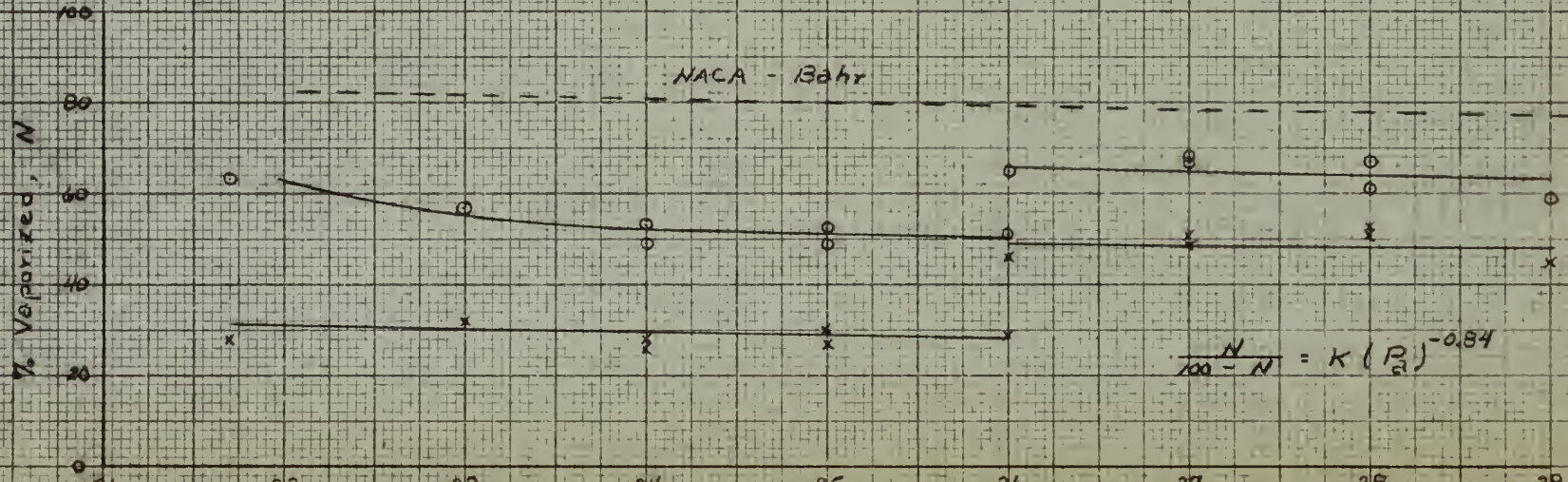

FIG 23a

INLET AIR VELOCITY INFLUENCE

P_2 = 27 In. Hg T_2 = 195°F.

F/A = .022 T_1 = 75°F

o Sta. 10
x Sta. 18

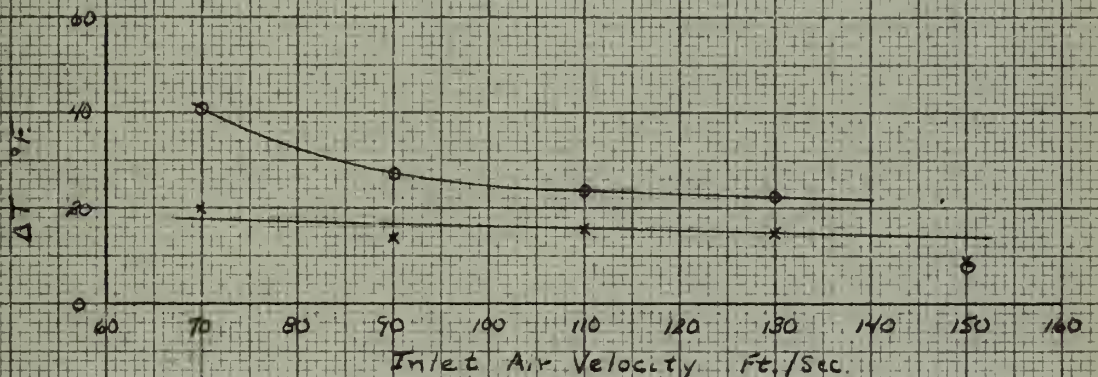

FIG 23b

$$\frac{N}{100 - N} = K(V_2)^{-1.43}$$

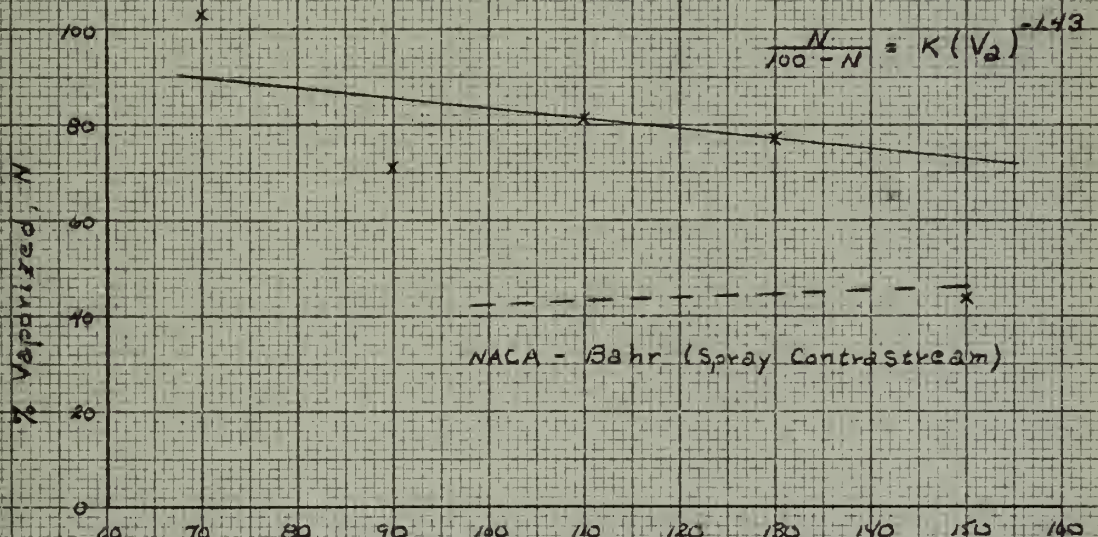

FIG 24a

FUEL - AIR RATIO INFLUENCE

T_2 = 325°F P_2 = 27 In. Hg

V_2 = 50 Ft/Sec. T_1 = 71°F

o Sta. 10

x Sta. 18

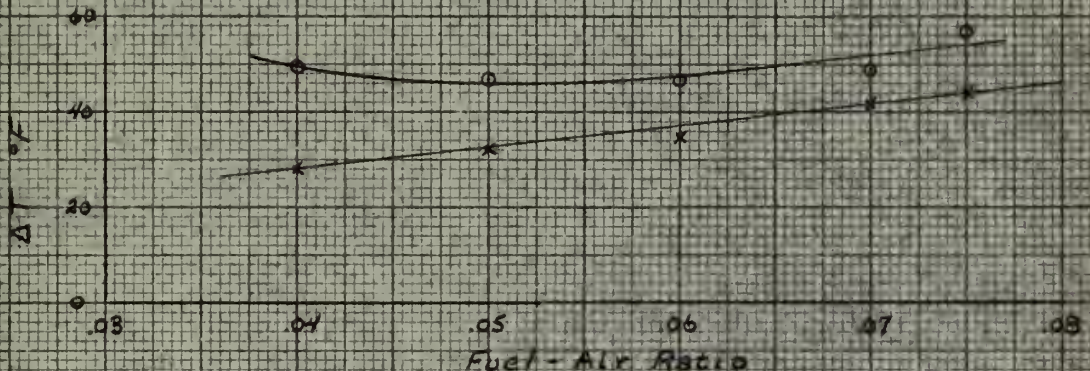

FIG 24b

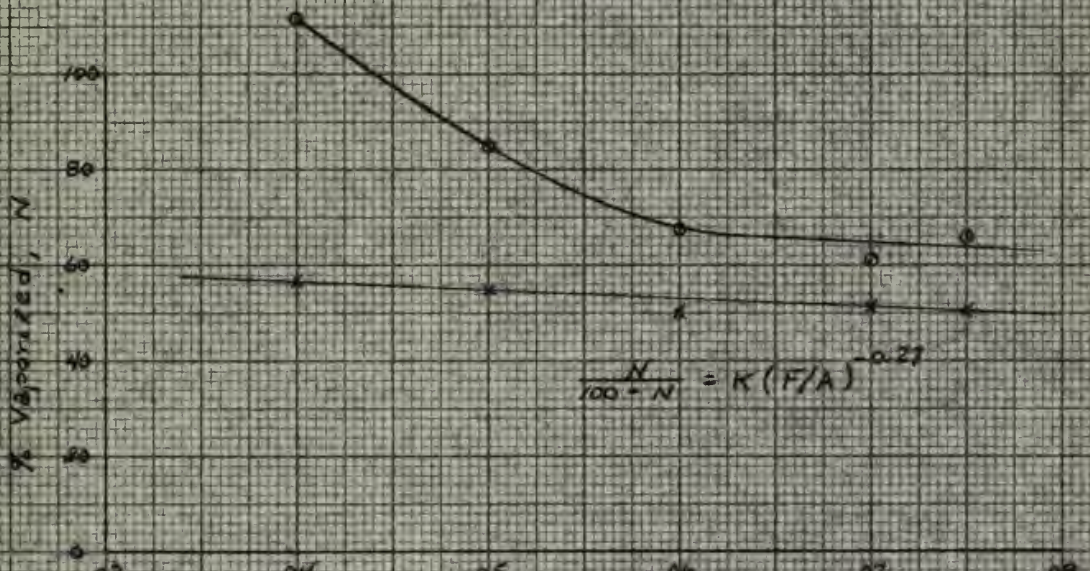

FIG 25

AXIAL DISTANCE INFLUENCE

T_b = 300°F V_b = 50 Ft./Sec.

F/A = .075 T_t = 74°F

P_a = 27 In. Hg.

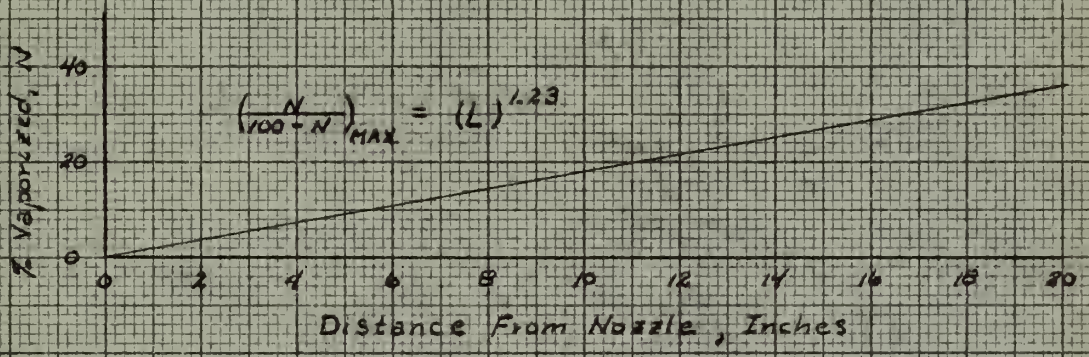

FIG 26

BENZENE WET BULB TEMPERATURE

(NACA T.N. 2368)

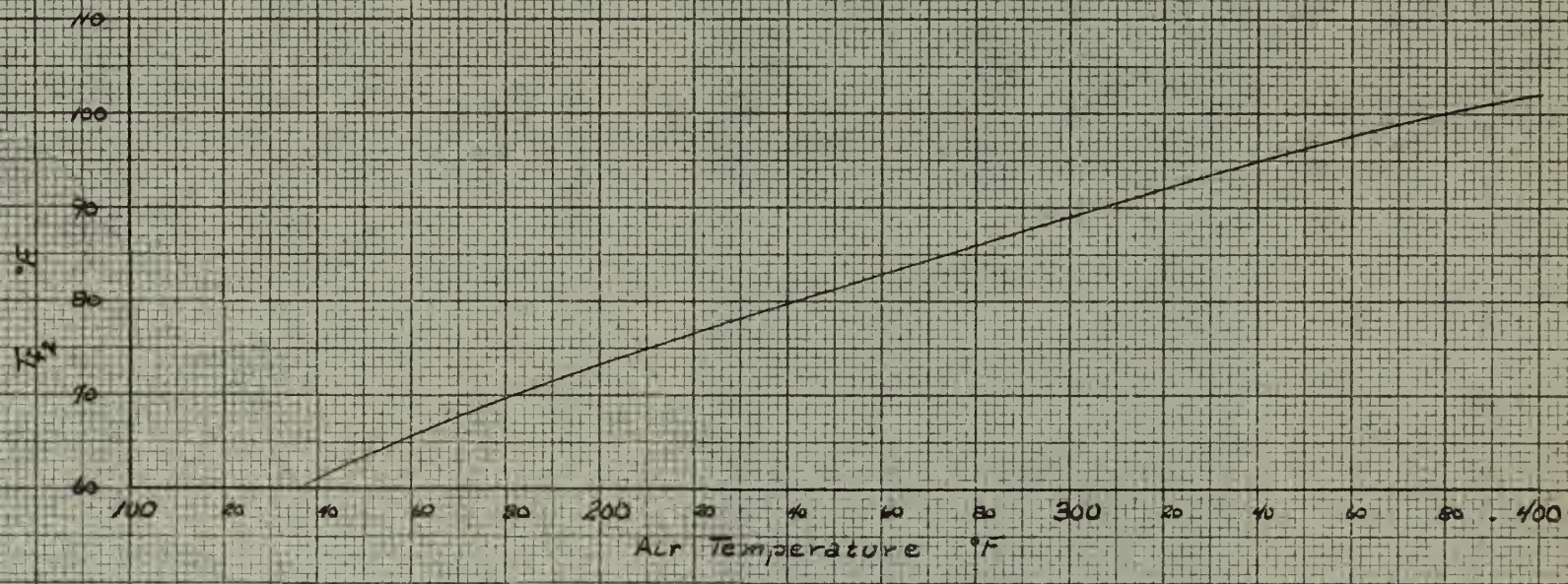

Fig. 27

Injector Nozzles

Appendix I

Calculation of Thermocouple Radiation Error

Ref. 5 gives the following equation for use when air is flowing normal to a single cylinder or wire:

$$\frac{h_c D}{k_f} = 0.32 + 0.43\left(\frac{DG}{\mu_f}\right)^{0.52} \qquad (1)$$

Equation (1) may be used for values of $\frac{DG}{\mu_f}$ from 0.1 to 1000. If an air temperature of 300°F is assumed,

$k = .013$ to 400°F

$\mu_f = .0581$

$\rho = .0522$

$V = 10$ ft/sec assumed flow past the wire inside the shield

$G = 1878$

$D = \frac{.020}{12} = .00167$ ft. diameter of the two wires together

Then:

$$h_c = 0.32\,\frac{k_f}{D} + 0.43\,\frac{k_f}{D}\left(\frac{DG}{\mu_f}\right)^{0.52}$$

$$= 2.49 + 26.8 = 29.3$$

Assume the emissivity of the thermocouple sensing element to be 0.7 and the temperature difference between the shield and the thermocouple is 100°F. From Fig. 27, page 63 of Ref. 5, h_r is equal to 2.0 for the assumptions. Then:

$$(t_g - t_p) = \frac{e h_r (t_p - t_s)}{h_c} = \frac{(0.7)(2.0)(100)}{29.3} = 4.78^\circ F$$

In the above example, the values were chosen to make the picture as bleak as possible and still the radiation error is small!

Appendix II

Method of Calculating Percent Fuel Vaporized

The heat balance equation for vaporization is:

$$\dot{m}_a c_{p_a}(T_{a_1}-T_{a_2}) = \dot{m}_f H_v X + \dot{m}_f c_{p_f}(T_{a_2}-T_{f_1})X + \dot{m}_f(1-X)c_{p_f}(T_{f_2}-T_{f_1})$$

which may be rewritten

$$(T_{a_1}-T_{a_2}) = \frac{F/A\ H_v X}{c_{p_a}} + \frac{F/A\ c_{p_f}(T_{a_2}-T_{f_1})X}{c_{p_a}} + \frac{F/A(1-X)c_{p_f}(T_{f_2}-T_{f_1})}{c_{p_a}}$$

Assume an inlet air temperature of 300°F, a fuel-air ratio of .075, a fuel inlet temperature of 75°F, and a temperature drop in the fuel spray of 45° so the air temperature read in the spray is 255°F.

$H_v = 170$

$c_{p_a} = .24$

$c_{p_f} = .42$

$T_{f_2} = 89°F$ from Fig. 26 for $T_a = 300°F$.

Then:

$$45 = \frac{(.075)(170)X}{(.24)} + \frac{(.075)(.42)}{(.24)}(255-75)X + \frac{(.075)(1-X)(.42)(14)}{(.24)}$$

$$45 = 53.1X + 23.6X + 1.8(1-X)$$

$$X = \frac{45 - 1.8}{76.7 - 1.8} = \frac{43.2}{74.9} = 57.6\%$$

Thesis
H523 Hess
c.1 Fuel vaporization in the pre-ignition zone of a gas turbine combustion chamber.
35882